University of Alberta

Adsorptive separation of C_2H_6 and H_2S from CH_4

By

Nicholas Brooks Kenneth Magnowski

A thesis submitted to the Faculty of Graduate Studies and Research in partial fulfillment of the requirements for the degree of

Master of Science

in

Chemical Engineering

Chemical and Materials Engineering

Spring 2014
Edmonton, Alberta

Abstract

The natural gas industry recognises that the need for removal of CH_4 from C_2H_6 feedstock C_2H_4 production and utilization. CH_4 being a contaminant in the production of C_2H_4 and furthermore in the production of polymers from C_2H_4. Dethanizers in gas processing plants are energy intensive and decreasing the energy from harvesting ethane from natural gas will improve the economics of C_2H_6 utilization. Na, Ba, and Ba/H exchanged forms of ETS-10 are investigated. Microwave radiation regeneration via desorption with H_2O is also investigated.

Precious metal catalysts that utilize natural gas must be protected from decreased efficiency and fouling due to H_2S contamination. This work proposes a guard bed method utilizing Zeoilite 13X, Cu-13X, Zn-13X, Pd-13X, and HiAl13X to remove the H_2S from a natural gas. These materials will be studied at room temperature to avoid the cost of heating a reactive bed such as the ones utilized in ZnO reactive operations.

Acknowledgements

First and foremost I wish to thank my supervisor Prof. Steven M Kuznicki, for his unwavering faith in me to get the job done, even when I doubted myself. Without the tremendous respect I have for him, and getting his approval as a top priority for me. I do not believe that this work would have been finished without his support. I spent a lot of time wavering on my decision to complete this work. At one point I had decided that I would not complete it and just move on, but the inspiring words of Dr Kuznicki kept me going.

I am also grateful for the help that members of our team gave me in the lab during the experimental phase of this work. Mrs. Weizhu Ann, Wu Lan, Tong, James Swada, Chris Lynn, David Kuznicki, and Meng Shi all deserve recognition.

I also need to express special thanks to my wife of 6 years for her tireless encouragement for me to finish this work. Also my parents who gave me financial support through times when having kids and a wife to support on a Masters Students Salary just wasn't enough. I had to take a professional position with GE because I got the offer and financially I needed to take the position. This lead to an extremely long and drawn out Thesis writing period of 4 years. Way too long in my opinion to complete this work but here we are and it is done.

Table of Contents

List of Tables

List of Figures

List of Equations

$$\frac{P}{x} = \frac{1}{x_m B} + \frac{P}{x_m}$$

$$x = \frac{P x_m}{\left(\frac{x_m}{K_H}\right) + P}$$

$$B = \frac{\alpha}{\beta\sqrt{2\pi mkT}} e^{\frac{Q}{RT}}$$

$$\alpha = \frac{K_{C_2H_6}}{K_{CH_4}}$$

$$C_g = \frac{C_{g1} - C_{g2}}{1 + e^{\left(\frac{x - t_{1/2}}{M}\right)}} + C_{g2}$$

$$C_g = C_{g2} - \frac{C_{g2}}{1 + e^{\left(\frac{x - t_{1/2}}{M}\right)}}$$

$$K = K_O e^{\frac{-\Delta U}{RT}}$$

Free Energy……..…….4

$$U = H - TS$$

Zero coverage Heat of Adsorption ……..4

$$\Delta H_0 = \Delta U_0 - RT$$

Microwave energy conversion into thermal energy……..…24

$$\tan\delta = \frac{\varepsilon''r}{\varepsilon'r}$$

Relaxation time…….……24

$$\tau = \frac{4\pi r^3 \mu}{kT}$$

Static dielectric constant limit……24

$$\varepsilon''r = \varepsilon'_{00} + \frac{\left(\varepsilon'_0 - \varepsilon'_{00}\right)}{\left(1+\omega^2\tau^2\right)}$$

High frequency dielectric constant……24

$$\varepsilon'r = \frac{\left(\varepsilon'_0 - \varepsilon'_{00}\right)\omega\tau}{\left(1+\omega^2\tau^2\right)}$$

Nomenclature

Abbreviations

BTU	British thermal unit
LLDPE	Linear low-density polyethylene
MDPE	Medium density polyethylene
HDPE	High-density polyethylene
NG	Natural Gas
C2-C5	Hydrocarbons with two to five carbons
PSA	Pressure swing adsorption
NGL	Natural gas liquids
GSP	Gas sub cooled
OHR	Overhead recycle
CRR	Cold residue reflux
RSV	Recycle split vapour
RSVE	Recycle split vapour with enrichment
TSA	Temperature swing adsorption
VSA	Vacuum swing adsorption
VPSA	Vacuum pressure swing adsorption
IGC	Inverse gas chromatography
HAP	Hazardous Air Polutants

MSA	Microwave Swing Adsorption
MEK	methyl ethyl ketone
ACFC	Activated Carbon Fiber Cloth
TCD	Thermal Conductivity Detector
SCD	Sulfur Chemiluminescence Detector
MEA	Monoethanolamine
DEA	Diethanolamine

Greek Letters

α	Limiting selectivity
	Sticking probablilty
PA	Pressure of a gas A
x	Amount adsorbed in the solid phase
x_m	Theoretical maximum amount adsorbed in the solid phase
B	Equilibrium constant
K_H	Henry's law constant
g	Gas denoted as g1 or g2
β	Rate constant for desorption
m	Mass

k	Boltzmann constant
R	Gas constant
T	Temperature
Q	Heat of Adsorption
C_{g1}	Minimum portion of the Boltzmann equation
C_{g2}	Maximum portion of the Boltzmann equation
$C_{g1/2}$	Location halfway between C_{g1} and C_{g2}
$t_{1/2}$	Location that corresponds to $C_{g1/2}$
M	Slope of the breakthrough portion of the Boltzmann curve
K_o	Pre-exponential factor
U	Internal energy
H	Enthalpy
S	Entropy
ε”r	Dielectric loss factor
ε’r	Relative permittivity
tanδ	Energy conversion from microwave to thermal
τ	Relaxation factor
r	Radius
μ	Dynamic viscosity

k	Boltzman's constant
ω	Angular frequency

Chapter 1

Literature Review

1.1 Introduction

The removal of C_2H_6 from CH_4 streams is of practical significance in the plasics industry. C_2H_6 purification has a stand alone benefit of improving the BTU and efficiency of natural gas use, but with too high an increace and the natural gas is not on specification. Through the removal of CH_4 hydrocarbons and the purification of the higher hydrocarbons such as C_2H_6, propane, and butane etc the use of the purified higher hydrocarbons C2-C5 can be optimised. The economic value of the C2-C5 hydrocarbons is much higher as they can be used to make much more valuable products such as polymers and resins. The removal of C_2H_6 specifically is of great importance in the polyethylene manufacturing sector. The production of Linear low-density polyethylene (LLDPE), medium density polyethylene (MDPE) and high-density polyethylene (HDPE) are produced from an C_2H_6 feed stock.[1] Pure C_2H_6 obtained from a NG source is the precursor for the C_2H_6 feed stock.

The removal of harmful H_2S is of great importance in the health and wellness of persons living near or at any petroleum refinery, natural gas well, or oil field service locations. The formation of aid gas also caused pipeline corrosion which can be costly to petrochemical companies which use extensive pipelining networks where the stream being transported contains H_2S. H_2S can also participate in the fouling of some catalytic centers which facilitate the conversion

of hydrocarbons into energy, the cost of maintaining catalyst is great. One alternative is the adsorptive removal of H2S from hydrocarbon streams. This can be performed in a conventional Pressure Swing Adsorption (PSA) unit through using zeolite 13X, or in order to get the selectivity to sufficiently low sulfur values a reactive material could be used that chemically reacts the H_2S and sequesters the sulfur. Such a material would benefit both low and high temperature operations.

1.2 Adsorption Fundamentals

A common term for adsorbent use in the separation of two different gasses is the selectivity. This is a value that is applied to a gas separation that recognises the preference a specific adsorbent has in adsorbing one gas over another. The symbol for selectivity is α_{g2}^{g1} and it is calculated as the capacity of one material for one gas (g1) over the capacity of another gas (g2) on that same material. The selectivity can be calculated from the Henry's Law constants which in turn can be obtained from the Langmuir Isotherm.

The Langmuir adsorption isotherm (equation 1, figure 1a), where the amount that is adsorbed in the solid phase is denoted as x and the pressure is denoted as P^{A}.[2]

$$\frac{P}{x} = \frac{1}{x_m B} + \frac{P}{x_m} \quad \text{.....(1)}$$

At high pressure where ad adsorbent becomes saturated with a gas, x becomes x_m which is defined as the theoretical maximum adsorption. B is the equilibrium constant or Langmuir constant which can be related to the Henry's

Law constant through the expression as $K_H = x_m B$, allowing the Langmuir equation to be expressed in a simpler form.

$$x = \frac{P x_m}{\left(\frac{x_m}{K_H}\right) + P} \quad \text{.....(2)}$$

The Langmuir constant shown as equation 3 is calculated from the sticking probability (α) also known as the accommodation coefficient for adsorption, which should not to be confused with the selectivity.[3] B is also calculated from the use of the rate constant for desorption (β), the mass (m) of the adsorbing molecule, the Boltzmann constant (k), the gas constant (R), the temperature (T), and the heat of adsorption $Q = -\Delta H$.[2]

$$B = \frac{\alpha}{\beta\sqrt{2\pi mkT}} e^{\frac{Q}{RT}} \quad \text{.....(3)}$$

The Henry's Law constants of two gases (in this case, C_2H_6 and CH_4) can be used to calculate the limiting selectivity (α) of an adsorbent for one gas over another as shown in equation 4. The Henry's Law constants were determined directly from the low pressure regions of each isotherm, where the Langmuir equation is reduced to a linear form also known as the Henry's Law form x = KP

$$\alpha = \frac{K_{C_2H_6}}{K_{CH_4}} \quad \text{.....(4)}$$

In this work the amount of gas adsorbed onto an adsorbent packed into a column is measured before the gas is detected at the outlet. When the gas is detected at the outlet of the column this is called breakthrough. The breakthrough curves were fitted to a best fit curve using the Boltzmann equation (equation 5,

figure 1.1b). The values of C_{g1} and C_{g2} are the minimum and maximum portions of the curve (before breakthrough and after breakthrough), $t_{1/2}$ is the value that corresponds to the x axis value at $C_{g1/2}$ which is directly halfway between C_{g1} and C_{g2}. M is the slope of the breakthrough portion of the curve.

$$C_g = \frac{C_{g_1} - C_{g2}}{1 + e^{\left(\frac{x - t_{1/2}}{M}\right)}} + C_{g2} \quad \text{.....(5)}$$

The Boltzmann equation was simplified for use in this work (equation 6), as the value of C_{g1} is zero.

$$C_g = C_{g2} - \frac{C_{g2}}{1 + e^{\left(\frac{x - t_{1/2}}{M}\right)}} \quad \text{.....(6)}$$

The Henry's Law constant is dependent on temperature as shown in equation 7. The K_o is a pre-exponential factor, and U is the free energy change associated with the exothermic process of adsorption U is negative along with H in equation 8.[3] Equation 8 also has the factor of entropy denoted as S. Equation 9 shows how to equate the heat of adsorption at zero coverage.

$$K = K_O e^{\frac{-\Delta U}{RT}} \quad \text{.....(7)}$$

$$U = H - TS \quad \text{.....(8)}$$

$$\Delta U_0 = \Delta H_0 - RT \quad \text{.....(9)}$$

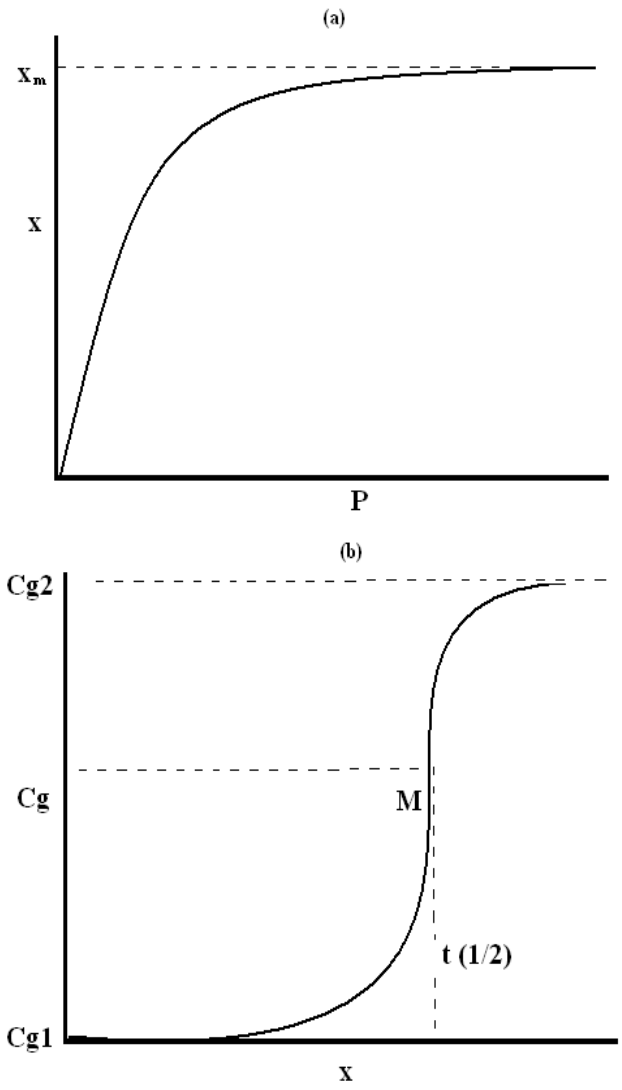

Figure 1.1 Graphical representation of the Langmuir equation (a) and the Boltzmann Equation (b).

1.3 Materials

1.3.1 Introduction

Zeolites are crystalline microporous aluminosilicates that are hydrated and are formed under high pressure in areas where alkaline lake beds once were situated. The temperature of the surroundings and the pH of the environment lead to different forms of mineral zeolites. The nature of the starting materials affect

the type of zeolite produced. Zeolites are microporous; they have a charged framework offset by cationic counterions. These cation's can have a +1 or a +2 charge and be available to ionic bond with active sites on the microporous framework. Water can reversibly adsorb to the surface of the framework throughout the structure. When these materials are dehydrated they are active toward gas adsorption and catalytic processes. Breck describes the synthesis of these materials from starting materials, nucleation and reaction time producing a myriad of microporous materrials.[5] In this work the use of ETS-10, and 13X was implemented therefore a short overview structure and synthesis of each will be considered.

1.3.2 ETS-10 Structure and Ion Exchange

All of the conventional zeolite materials, which are one type of micorporous framework solids, have tetrahedrally coordinated metal atoms, and have some value of Si/Al. There are 206 framework types of zeolites that have been discovered and among them 60 naturally occur as sedimentary mineral deposits. The Si/Al ratio determined the amount of Al^{3+} that exists in the material and can infer the capacity for ion exchange. The titanosilicates class of microporous materials have an octahedral coordinated titanium atom which is linked through oxygen (O) bridges and are in a straight chain. The Si atoms which are tetrahedrally corrdinated are bound to the Ti atom forming two three ring structures.[6] These titanoslicate frameworks are built upon a corner-sharing system of T_iO_6 octahedra and SiO_4 tetrahedra. The titanium chains are linked up

perpendicularly to chains of the same type. This forms rings of seven members, and through stacking of these rods apicaly and axially 12 member rings are formed. These 12 member rings forms have the dimensions of 7.6 x 4.9A.[6] Dislocations exist within the structure resulting in micropores having a size of 14.3 x 7.6 A, this is due to the shifting of ½ a unit cell over.[6]

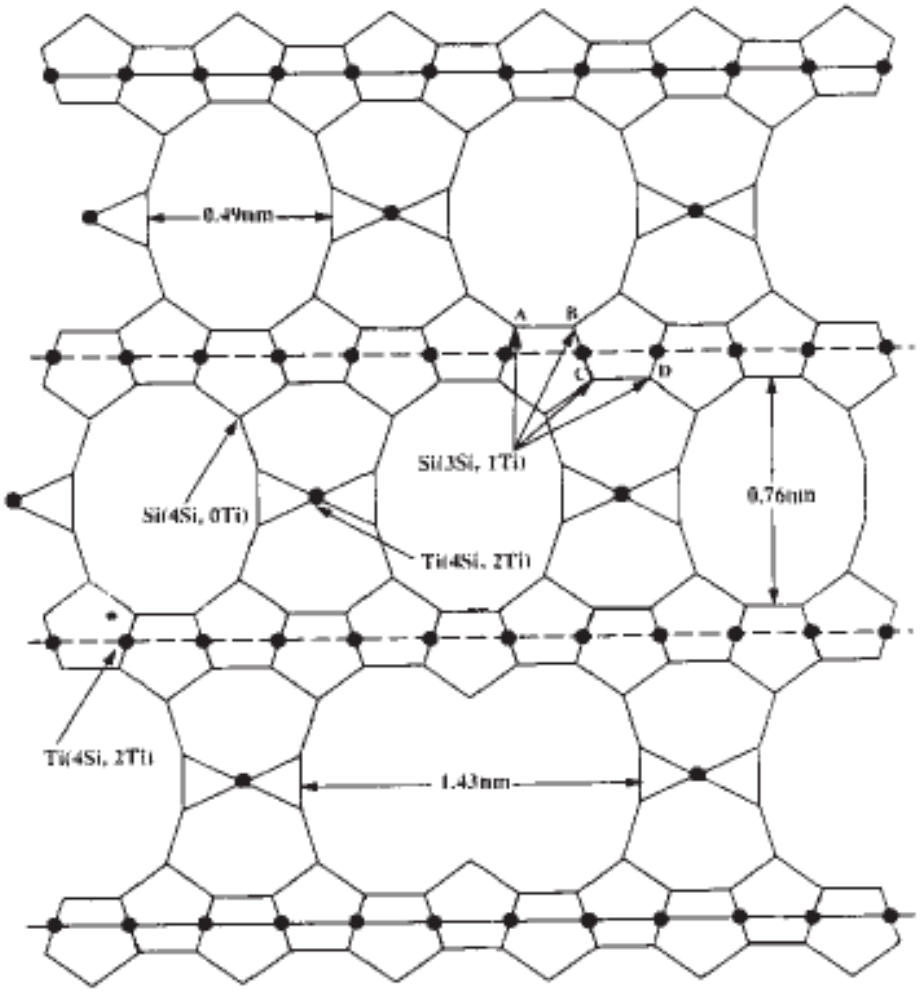

Figure 1.2 The structure of ETS-10 showing a stoichiometry of $Si_5Ti_{13}^{2-}$.[6]

ETS-10 has been documented to have the ability to exchange the active sites on the framework with a number of cations. Schmidt et all have exchanged $NH4^+$, K^+, Na^+ and Cs^+ atoms into the structure of ETS-10.[7] Nastro et all have exchanged as well as characterized the structure of ETA-10 exchanged with Na^+, K^+, Li^+, Mg^{2+}, Ca^{2+}, and Cu^{2+}.[8] The adsorptive properties of ETS-10 in various exchanged forms have also been studied. Adsorption of C_2H_6 and C_2H_4 onto Ag^+, Na^+, K^+, Li^+, Cu^{2+},Ba^{2+}/H^+, and Ba^{2+} ion exchanged variations of ETS-10 has been studied.[9] The Na^+, K^+, and Ag^+ forms were found to adsorb both C_2H_6 and C_2H_4 strongly showing a sharp rectangular adsorption isotherm. Methane adsorption has been studied by Loughlin et all on the native form of ETS-10.[10]

The ease with which ETS-10 can exchange cations is shows in a study where heavy metal exchanged versions have been produced with Pb^{2+}, Cd^{2+}, and Cu^{2+} on ETS-10 membranes to determine the effectiveness these membranes could have in the removal of these heavy metals from water.[11] ETS-10 has also been used in catalysis studies. Exchange with ammonium has been previously documented.[12] The local structure of ETS-10 through Ion exchange with NH_4^+ has resulted in damage to the ETS-10 structure. This damage is in the form of protons attacking the framework due to decomposition of the ammonium cations on the polar sites.[13,14] This produces Hydrogen from ETS-10.

Ag^+ exchange is useful in the separation of Propane from Propylene where the Ag-ETS-10 is more selective toward propylene.[15] The Ag^+ form of ETS-10 could also be utilized as a bactericidal agent by reducing the exchanged Ag-ETS-10 with $NaBH_4$ insitu.[16]

1.3.3 Zeolite 13X

Zeolite X which is widely known as 13X can be synthesised from Sodium Aluminate-Sodium Silicate Gels as a variation on the molar ratios of the components in the following system. Molar components of the system Na_2O-Al_2O_3-SiO_2-H_2O are used to create gels where crystallization of the gels can occur under specified conditions.[5] Gels of the molar ratio 3.6:3:144 for a ratio of Na_2O:SiO_2:H_2O are used. Typically the Na-X form of this material is formed and there are four sites that the Na^+ cations are found. The roman numerals from figure 1.3 represent sites where the extraframework cation positions are situated. These sites have 32 Na^+ cations in sites I$^/$, and II, as well as 28 Na^+ cations in two separate III$^/$ sites.[17] Zhu et all have indicated in figure 3 that the atoms of nonequivalent Oxygen are indicated as the numbers 1-4. There is a small window of values with which to judge whether a particular material is Zeolite X or another form. It has been found that Zeolite X has 4% of the Al atoms in the crystal structure substituted as Si atoms. The parent structure seen in figure 3 is of faujisite which is a parent compound of Zeolite X, i.e. Zeolite X can be synthesised from that parent compound, which is a mineral Zeolite. The size of the pores i.e. the 12 member ring tunnels diameter is approximately 7.4 A. The non-equivalent oxygen atoms are indicated by the numbers 1-4.[12] Silicon and aluminum atoms alternate at the tetrahedral intersections except that Si substitutes for Al at about 4% of the Al positions in the crystal studied. Extra framework cation positions are labelled with Roman numerals.

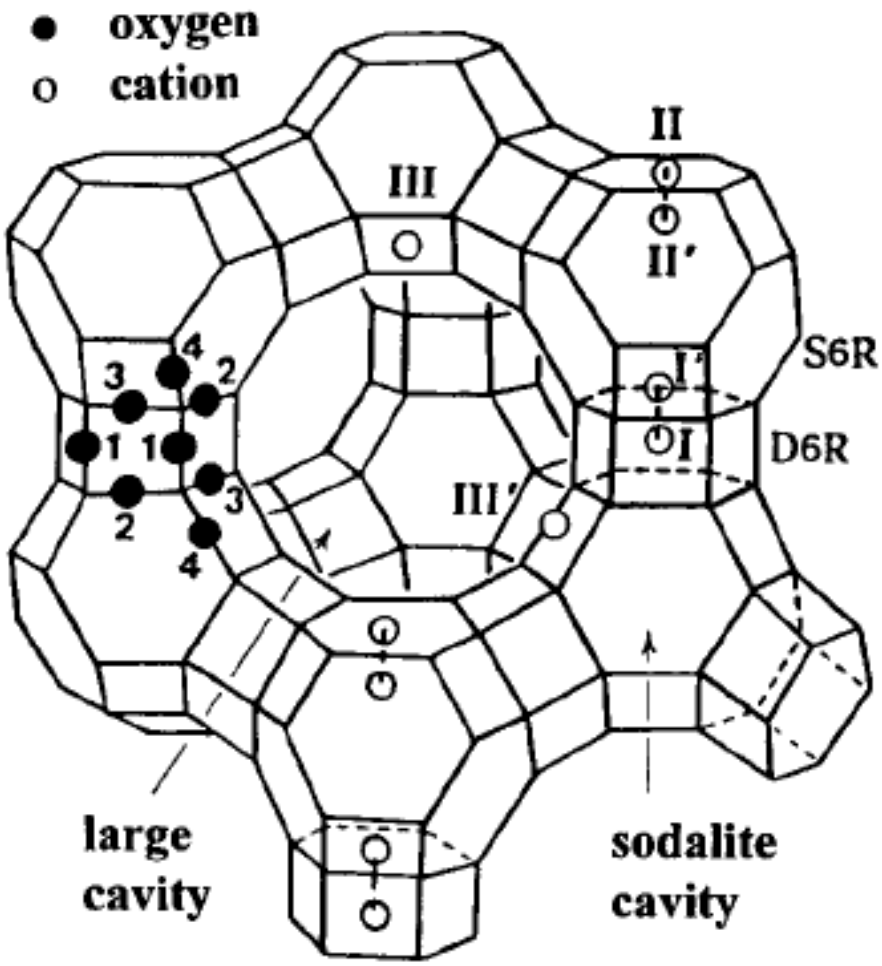

Figure 1.3 Stylized drawing zeolite X framework. Oxygen atoms exist at the center of each line segment.[17]

1.4 Historical Perspective on conventional C_2H_6/CH_4 Separations

1.4.1 Introduction

Purification of CH_4 from natural gas liquids (NGL) is economical due to the high energy output of CH_4 with relation to its carbon footprint. With NG being a commodity cost of processing and market price play a heavy role in the technology used. Removal of NG contaminants such as H_2S, CO_2, and N_2 increace the energy obtained. The capture of the C_2H_6 from NGL is also economical in the plastics industry. The C_2H_6 is a precursor for the production of C_2H_4. The production of C_2H_4 is performed in a catalytic cracker. C_2H_6 is the preferred feedstock to C_2H_4 plants because the efficiency is highest. The cost of production of ethylene is lowest when using a lower carbon NG product. Higher carbon NG constituents such as C_3H_8, C_4H_{10}, and C_5H_{12} can be used, but this increases the cost. These higher carbon constituents have a higher value separately. Removal of the higher carbon components also prevents fouling of downstream piping. Conventional cryogenic separation techniques are energy intensive due to the high compression power. This is discussed in the next section.

1.4.2 Separation of CH_4 and C_2H_6 a Historical Perspective.

Conventional Separation of CH_4 and C_2H_6 from NGL is performed through cryogenic separation. Up to 1998 Efficient NGL recovery from NG conventionally has been performed by a process called the Gas Subcooled Process (GSP) developed by Ortloff shown in figure 1.4a. In this process some of the feed gas is subcooled and added to the top of the as feed, this facilitates the capture of

the C_2+ components of the NGL's.[18] An additional process called the OverHead Recycle Process (OHR) was developed.[18] Figure 4b shows the OHR process. This additional component to the GSP employs the recovery of the vapour stream at an intermediate point and it is added to the top of the composite tower. This added component is great for the recovery of C_3+ components but reduces the C_2H_6 recovery.[18]

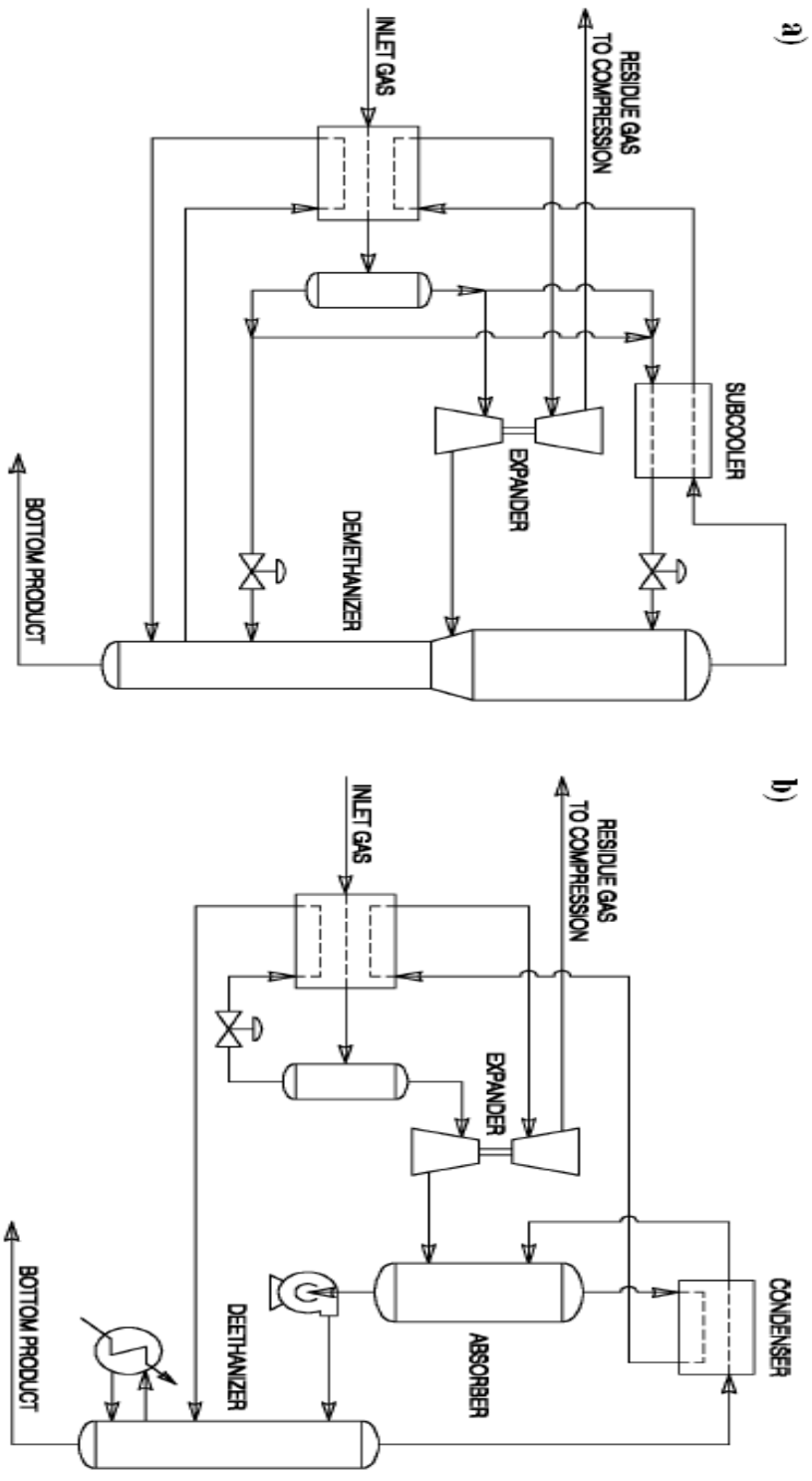

Figure 1.4 Process design for the Gas Subcooled Process (GSP) (a), and the OverHead Recycle Process (OHR) (b).[18]

In the sub cooled split vapour stream there exists available refrigeration. Utilizing this refrigeration availability the Cold Residue Reflux process (CRR) was formulated. This process allows for greater C_2H_6 recovery in utilizing a CH_4 reflux stream which has been compressed to a greater extent than in the GSP and rectifying the tower vapours more efficiently. Also the split vapour line provides the bulk of the C_2H_6 recovery. The Recycle Split Vapour process (RSV) was also proposed where it is similar to the CRR but with the added residue gas recycle through the subcooler and added to the top of the tower.[18] An added benefit to both the RSV and the CRR is that C_2H_6 recovery can be switched to C_2H_6 rejection in order to curtail market fluctuations. Further research resulted in the development of the Recycle Split Vapour with Enrichment process (RSVE). In this process the split vapour stream is mixed with the recycle stream before being subcooled.[18]

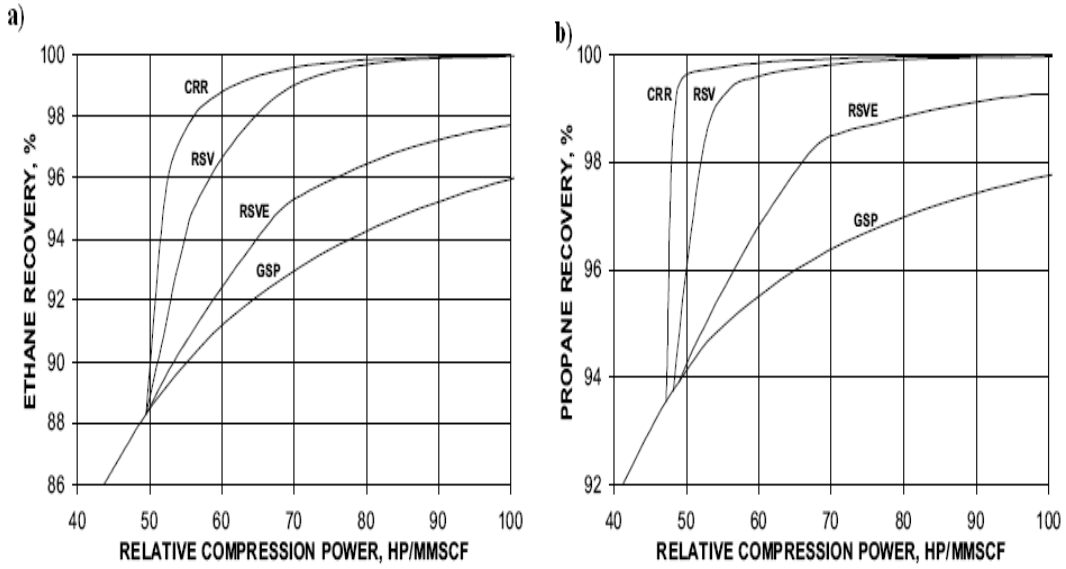

Figure 1.5 The comparison of the C_2H_6 recovery performance (a) and the C_2H_6 rejection performance (b).[18]

C_2H_6 recovery is most important in the production of plastics, therefore a good basis to judge all of the aforementioned processed is to compare based on the C_2H_6 recovery vs the compression power, which relates to the energy requirement. Figure 1.5 shows a comparison of all processes mentioned with respect to C_2H_6 recovery and C_2H_6 rejection. The CRR process shows the greatest recovery with the lowest relative compression power. For instance if the C_2H_6 recovery is 92% then the compression power is 20% lower than the basic GSP design. Shown in figure 1.6 is the process design for the CRR type with the highest performance.

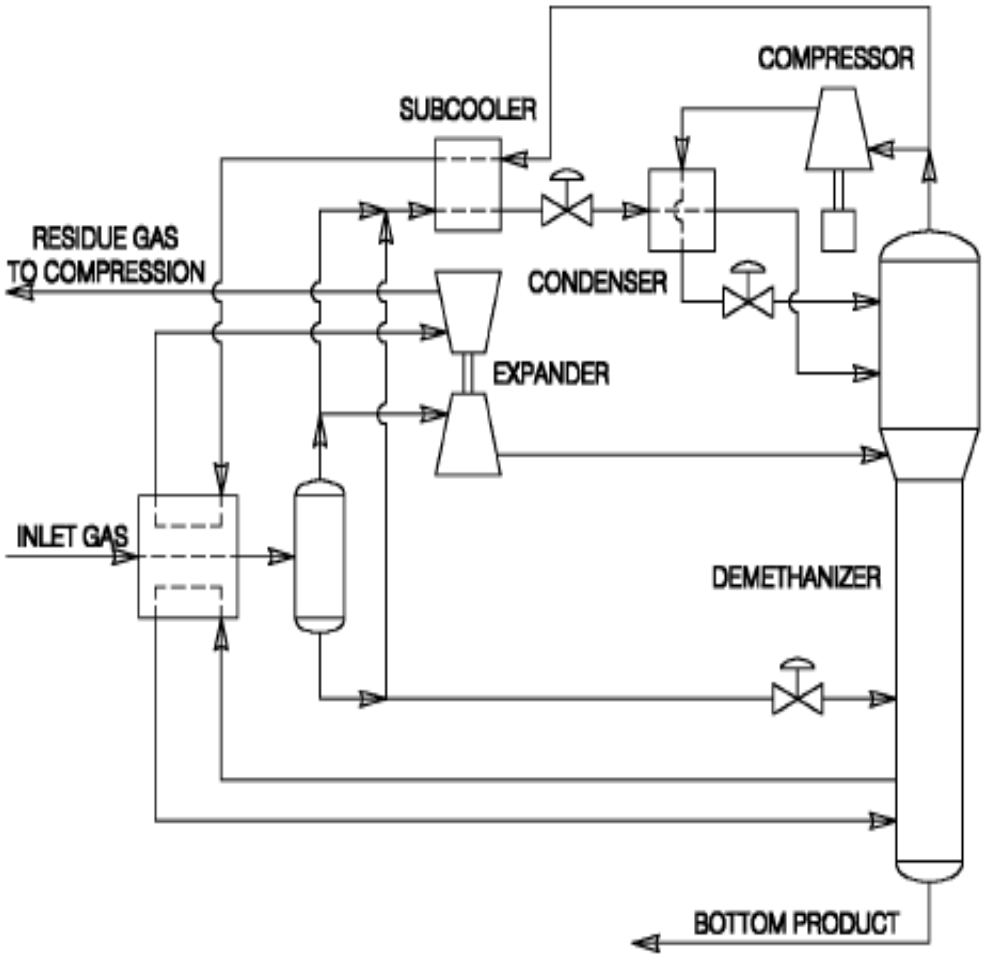

Figure 1.6 The process design for the CRR process.[18]

1.5 Pressure Swing Adsorption

1.5.1 Introduction

The separation of C_2H_6 from CH_4 streams as mentioned before can be done through cryogenic separations and discussed in this section is an alternative method through use of adsorbents in a pressure swing system (PSA). PSA is an attractive alternative to cryogenic distillation because the compression requirements to achieve the separation of two or more components are typically lower. One PSA process that can be highlighted here is the skarstrom cycle. In the skarstrom cycle there are 4 steps. During Step I of the process the gas mixture is passed through an adsorbent bed at high pressure. After a unit length of time which facilitates a pure stream of the desired product is met the column is then cut off from the feed stream. In step II the pressure is then reduced to a defined level countercurrently i.e. in the opposite direction of the feed stream. The desorbed gas being the unwanted component of the gas mixture is then removed as the pressure is decreased to a defined level. Step III is where the low pressure level is met, the column is purged with clean product gas and re-pressurised. The final step is step IV where the re-pressurisation is performed by supplying a fraction of the product gas to the front of the column and co current flow of the product recycle in order to set up the adsorbent with a saturated state. This sets up the adsorbent with pore filling and void filling of the more preferentially desired gas and less strongly adsorbed gas. If the desorbed gas is enriched with the unwanted more strongly adsorbed gas then the separation is effective. In the case of C_2H_6 from CH_4 separation as we will discuss later in this work the more strongly adsorbed species would be the more highly valued or wanted gas. In relationships such as these a

Vacuum Swing Adsorption (VSA) or a Vacuum Pressure Swing Adsorption Cycle (VPSA) is utilized. The fundamentals of PSA and Vacuum steps are similar to what has been described. Dropping the pressure low enough to remove the more strongly adsorbed species is the differing step. Schuab and Smolarek have developed a VSA cycle.[22] Figure 1.7 shows a diagram representation of the 4 steps of the skarstrom cycle.

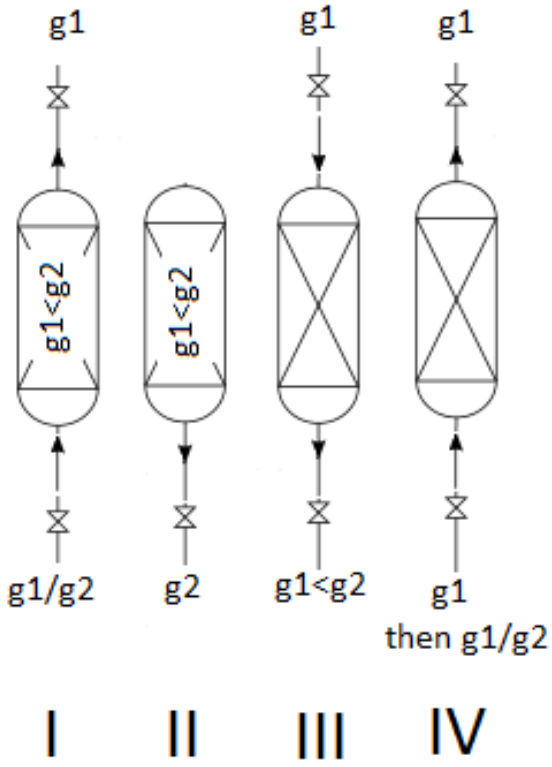

Figure 1.7 A diagram representation of the 4 steps of the skarstrom cycle where gas g2 is the more strongly adsorbed species over g1. Step I pressurisation, step II countercurrent depressurisation, step III purge, and step IV re-pressurisation.

The time to breakthrough of the more strongly adsorbed gas during step I is determined through study of the particular adsorbent and it's α of one gas other the other. Shown in figure 1.8 is a representative diagram of what the adsorption front and desorption front might look like.

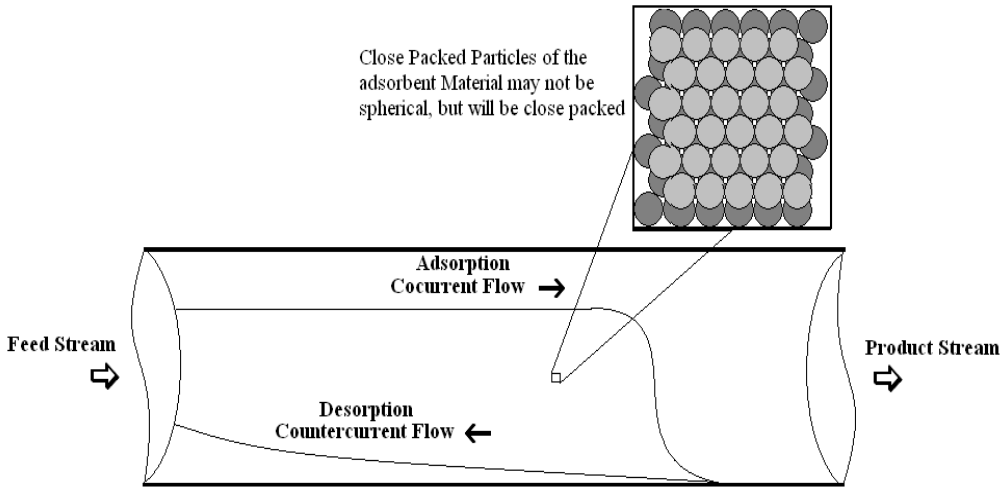

Figure 1.8 A representation of the Adsorption and Desorption profile of the adsorbent bed used in PSA processes.

1.5.2 C_2H_6/CH_4 Separations a materials perspective

Materials such as Activated Carbon, Zirconium oxide pillared clay, 4A, CaX, 13X, 5A, Silicalite-1, have differing selectivity (α) towards C_2H_6 over CH_4.

On Activated carbon $\alpha_{CH_4}^{C_2H_6}$ can be calculated from the values of x_m and B where $K_H = x_m B$ and K_H for CH_4 is 9.055.[19] The value of K_H for C_2H_6 is 102.05.[19] The selectivity is then calculated as $\alpha_{CH_4}^{C_2H_6} = K_{H,C_2H_6} / K_{H,CH_4} = 11.27$ at 293.15K. Brotas de Carvalho et all studied the adsorption of CH_4 and C_2H_6 on Zirconium

oxide pillared clays.[20] Two different deposits of the raw one from the Benavila–Alentejo (BEN) deposit and the other from the Porto Santo Island –Madeira archipelago (PTS) deposit. From this work observations made about the $\alpha_{CH_4}^{C_2H_6}$ were that it decreases significantly with temperature and less so at high pressures up to 100 KPa.

Khulbe et all have reported separation results from a gas chromatographic method for C_2H_6 and CH_4, but focusing on the separation of C_2H_4 and propane from C_2H_6 and CH_4.[21] The materials used in this study were H-mordenite and 13X, CaX, 4A and 5A zeolites. The results for C_2H_6 and CH_4 show that the separation is possible. The Henry's Law values for C_2H_6 and CH_4 on 4A and 5A are shown in Table 1.1. Accurate determination of the selectivity for C_2H_6 over CH_4 is difficult to determine from these results but it is shown that there is a significant Henry's constant difference between the two. Adsorption information on the H-mordenite, 13X, and CaX was not determined for C_2H_6 therefore adequate information in determining the separation parameters is lacking. This work determined that separation is possible but the need for more data specifically retention time and ΔH_0 to calculate henry's law constants. Equations 7 and 9 above describe the math needed to calculate the henry's law constants. Silicalite-1 adsorption of CH_4 and C_2H_6 was studied at 305 K for C_2H_6 and at 304 K for CH_4.[22] The Dubinin-Polanyi equation was used to fit the data for each isotherm.[18] The data showed that C_2H_6 had the highest heat of adsorption as that compared to CH_4, also the heat of adsorption for C_2H_6 did not change much with adsorbate loadings as compared to the decrease in heat of adsorption for CH_4 with increased

adsorbate loadings.[18] This leads us to understand that with increased adsorbate loadings leading to a decrease in the heat of adsorption of CH_4, CH_4 can be easily removed from an adsorbate at increased adsorbate loadings. This is however not the case with C_2H_6. Therefore with high adosrbate loadings the yield of CH_4 can be high with a regeneration step being energetically equivalent to remove C_2H_6 at low adsorbate loadings. Table 1.1 shows the calculated selectivity values at 298K for all of the adsorbents mentioned in this section. A comparison of these selectivity's with the materials used in this study will be made in chapter 2.

	Selectivity ($\alpha_{CH_4}^{C_2H_6}$) at 298K
Activated Carbon	10.5
5A	23.5
4A	38.0
Zr-PTS	8.0
Zr-BEN	7.0
Silicalite-1	N/A

Table 1.1 Selectivity's at 298K of C_2H_6 over CH_4. Materials include Zeolite 5A, Zeolite 4A, Zr-PTS, Zr, BEN, activated carbon, and Silicalite-1.[20,21,22]

1.6 Temperature Swing Adsorption (TSA)

TSA is similar to PSA in that there is an adsorption step and there is a separation of two or more gasses. The main difference is that during the regeneration step an increace in temperature is used to obtain the more preferentially adsorbed species. During PSA there is no temperature increace in order to regenerate. The increace in Temperature from T_1 to T_2 decreaces the loading from x_1 to x_2. Figure 1.8 shows a representation of an isotherm graph that displays the difference between two different temperatures in a TSA process and the effect that a different temperature has on the adsorbent loading. Typically in a commercial process a purge gas is utilized that is heated during the desorption thermal heating step that demarcates TSA from PSA. TSA offers advantages when the preferential gas is the more strongly adsorbed species. Also with a small change in temperature there is a possibility to recover a large quantity of adsorbate i.e. small ΔT large Δx.

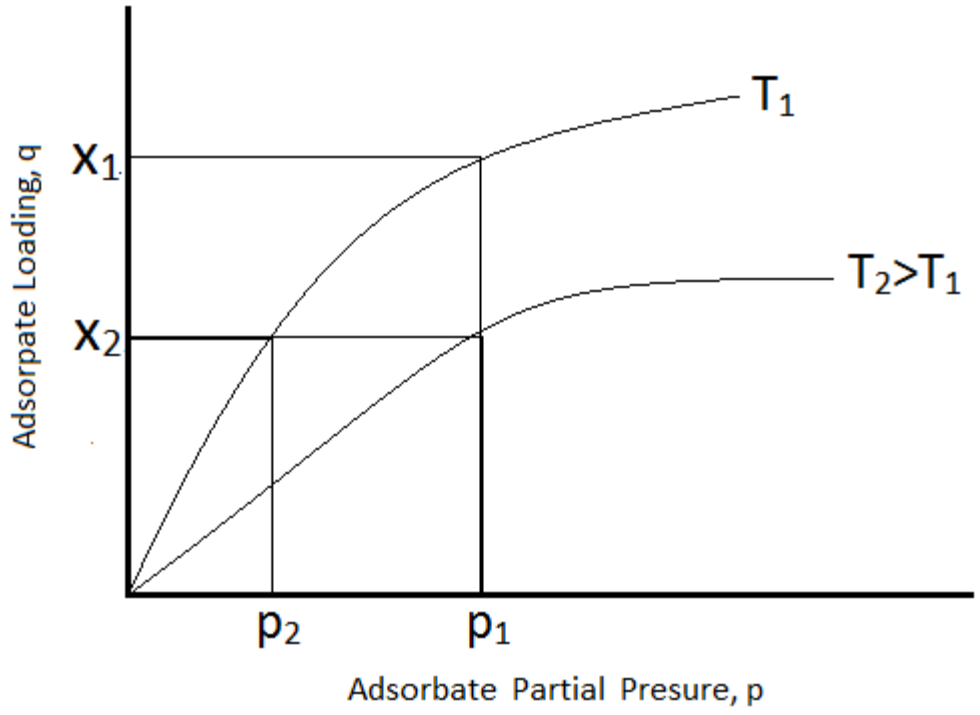

Figure 1.9 Isotherms at T1 and T2 showing the difference in adsorbate loadings and partial pressures.

1.7 H_2O Desorption and Microwave Regernation

Microwaves which exist in the range of 0.3-300GHz of the electromagnetic spectrum can offer an effective method of regeneration of a saturated adsorbent. Through the action of dielectric heating, a material can increase its internal energy thorough the adsorption of microwave radiation. The conversion of microwave energy to internal thermal energy is directly related to the dielectric properties of the material. The heating of a material with use of 0.3-300MHz radiation occurs through dipolar polarization and conduction losses. The following is an analysis of the physics of dielectric heating.[23]

Microwave energy conversion into thermal energy is represented as tanδ which is the ability a material has for the energy conversion. And ε"r is the loss factor which measures the ability a dielectric material has in converting the microwaves into heat. Also ε'r is the relative permittivity which measures the polarizability of a material under the influence of an electric field. Equation 10 shows the relationship between the conversion to thermal energy by the material, the polarizability of that material and the loss factor.

$$\tan\delta = \frac{\varepsilon''r}{\varepsilon'r} \quad \text{.....(10)}$$

The relaxation time τ for a spherical dipole is represented as follows in equation 10. In equation 11, r is the radius of the dipole, μ is the dynamic viscosity, k is the Boltzman's constant, and finally T represents temperature. Various materials will have different ε"r, and ε'r values which depend on the angular frequency ω = 2πf and the relaxation time τ. The limits of the dielectric constants are represented as ε'_0 and ε'_{00} which are the static and high frequency constants. Equations 12 and 13 show the relationship between relaxation time, static and high frequency constants, and the angular frequency for ε"r, and ε'r values.

$$\tau = \frac{4\pi r^3 \mu}{kT} \quad \text{.....(11)}$$

$$\varepsilon''r = \varepsilon'_{00} + \frac{\left(\varepsilon'_0 - \varepsilon'_{00}\right)}{\left(1+\omega^2\tau^2\right)} \quad \text{.....(12)}$$

$$\varepsilon'r = \frac{\left(\varepsilon'_0 - \varepsilon'_{00}\right)\omega\tau}{\left(1+\omega^2\tau^2\right)} \quad \text{.....(13)}$$

The polarization of the dipole occurs only in polar compounds such as H_2O, and CH_3OH. Through exposure of polar molecules with an oscillating electromagnetic field such as microwaves the neibouring water molecules will agitate one another as they align themselves with the external field. In the case of water this process produces internal thermal energy and thus facilitates a phase change from liquid to vapour. Shown below in figure 1.9 is a schematic drawing of what occurs when microwave radiation penetrates water molecules, emphasis is put on the changing direction of the dipole moment which is the basis for thermal energy generation.

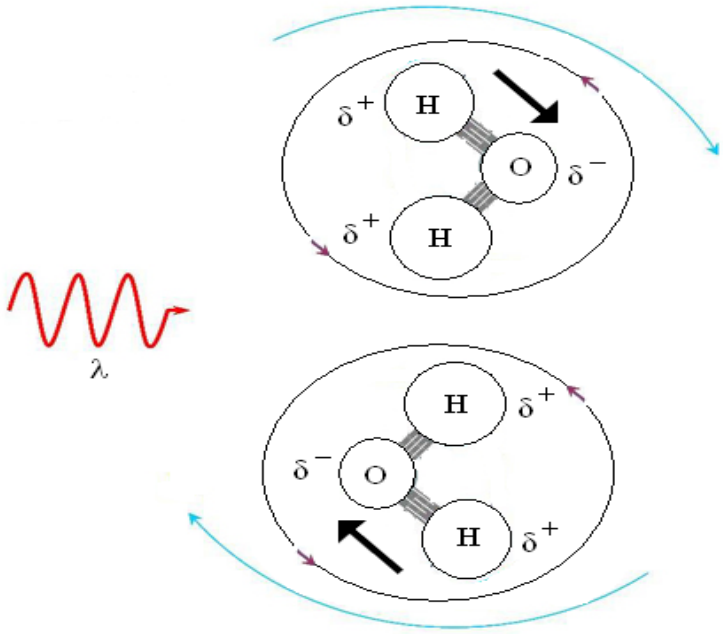

Figure 1.10 A figurative representation of what physical changes take place during microwave heating of a water molecule.

Microwave Swing Adsorption (MSA) has been studied from the removal of VOC's, which can be polar organics, and Hazardous Air Polutants (HAP's.[24]

The HAP's studied in this work were water, methyl ethyl ketone (MEK), and tetrachloroethylene which all have dipole moments thus would be suitable for microwave desorption. Figure 1.10 shows a schematic or the MSA system used in this study. The power supply to the microwave generator was pulsed in order to regulate the internal temperature of the Activated Carbon Fiber Cloth (ACFC) adsorbent, and results indicate successful regeneration with collection efficiencies of 99.8%.

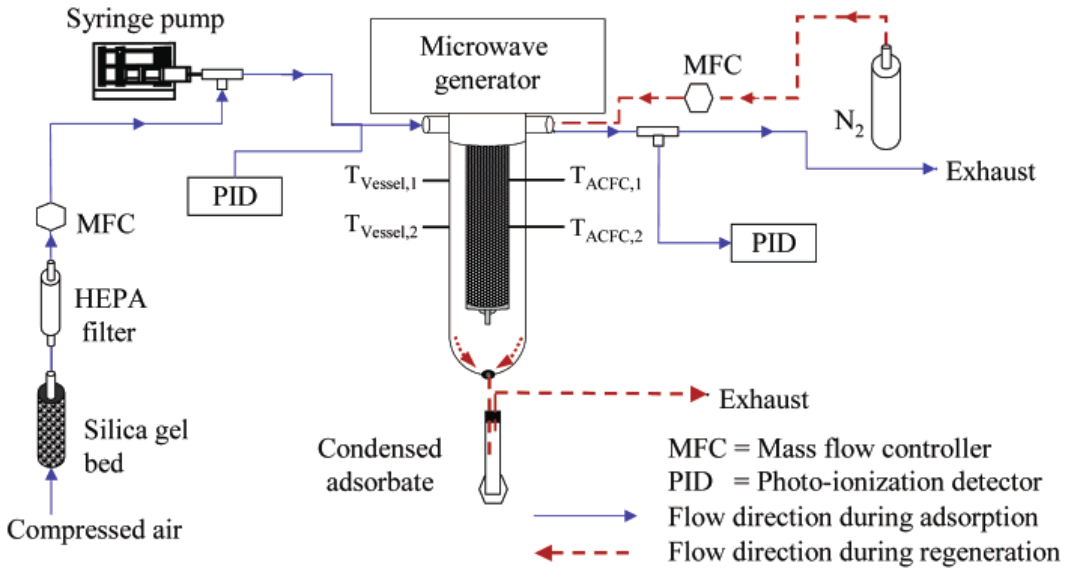

Figure 1.11 A process schematic of the MSA unit implemented by Hashsho et al.[24]

Considering ETS-10 microwave conductive heating has been used to regenerate the Na form to desorb C_2H_6/C_2H_4 and CO_2/CH_4 mixtures. Heat was transferred to the adsorbent via heating tape for the conductive heating portion, and microwave radiation was applied to the adsorbent for the microwave portion. Microwave heating showed a much quicker desorption rate compared to the conductive heating for the C_2H_6/C_2H_4 mixture. For that same mixture the cooling time was also much quicker by

a factor of 3. Considering the gas recovery again for the C_2H_6/C_2H_4 mixture the microwave heating was superior. Microwave heating produced 96% gas recovery for the as opposed to the 74% gas recovery for the conductive heating. For the CO_2/CH_4 mixture heating time and cooling time were comparable and gas recovery was 74% for microwave heating, and 61% for conductive heating.

Other forms of microwave regeneration via indirect and direct heating have been studied on Na-ETS-10.[25,26] Direct microwave heating is the same as mentioned above, but indirect microwave heating is through saturating the adsorbent with H_2O before regeneration. The gas recovery when desorbing a mixture of CO_2/CH_4 was 100% initially, but after successive cycles this value dropped as low as 18. For the direct microwave regeneration gas recovery was 40% and improved after successive cycles as high as 55%.

1.8 Scope of thesis

This work at the outset was a study designed to determine effective removal of C_2H_6 from CH_4. This separation is important in the production of C_2H_4 in that C_2H_6 is a nessesary feed stock for cracking and producing C_2H_4. C_2H_4 is a precursor for the production of polymers of many types. It was nessesary to use multiple techniques to determine the effectiveness that materials studied in this work have in the removal of C_2H_6 from CH_4 and further from C3's, C4's and C5's. Isotherm collection, (IGC) Inverse gas chromatography and the collection of breakthrough curves were all nessesary in determining the selectivity and efficiency in the removal of C_2H_6 from CH_4. In the desorption of C_2H_6 from ETS-10 materials

i.e. regeneration, the use of microwaves was implemented where the nessesary energy of the conversion of a saturated bed of ETS-10 to an activated state free depleted of adsorbed C_2H_6. This desorption process is nessesary in the formation of a cycle which can be used in industrial applications for the removal of C_2H_6 from a natural gas stream.

Another aspect of this work was to determine which adsorbents/reactive materials can be usefull in the removal of H2S from a natural gas mixture. This separation is usefull in many applications but of specific importance to this work is the removal of H_2S for use in a guard bed for precious metal catalytic units. The H_2S is a poisoning agent on the surface of the catalyst and its effective removal would mean a reduced budget for many end users of the catalytic bed.

[1]Nova 2009: http://www.novachem.com/Locations/locations_joffre.cfm

[2]Langmuir, I., 1916. The Evaporation, Condensation and Reflection of Molecules and the Mechanism of Adsorption. Physical Review 8, 149-176

[3]Yang. R.T., 2003. Adsorbents Fundamentals and Applications, A John Wiley and Sons, inc., Publication, University of Michigan.

[4]Kneabel. K. S., Farooq. S., Ruthven. D. M.; Pressure Swing Adsorption.

[5]Breck, D.W., 1974. Zeolite Molecular Sieves: Structure, Chemistry and Use. Wiley-Interscience Publication, John Wiley & Sons, London.

[6]Anderson, M.W., et al., 1994 Structure of the microporous titanosilicate ETS-10, Nature 367, 347-351.

[7]Schmidt, W,. et all,. 2007. On the influence of ion exchange on the local structure of thetitanosilicate ETS-10. Physical Chemistry Chemical Physics 9. 3440–3446

[8]Nastro, A,. et all,. Characterisation of ETS-10 and ET(FE)S-10 molecular sieves exchanged with different cations. Environmental Engineering and Management Journal. Vol.3. No.3. 231-238

[9]Anson A, et al., 2008. Adsorption of ethane and ethylene on modified ETS-10. Chemical Engineering Science 63, 4171-4175.

[10]Cavalcante, C, L,. 2000. Industrial Adsorption Separation Processes: Fundamentals, Modeling and Applications. Latin Americal Applied Research. (30). 357-364

[11]Jiang, J.W., et al., 2009. Exchange of heavy metal ions in titanosilicate Na-ETS-10 membrane from molecular dynamics simulations, Journal of Membrane Science 335, 89-95.

[12]Doren, D.J., et al., 2009, Photocatalytic oxidation of ethylene by ammonium exchanged ETS-10 and AM-6. Applied Catalysis B: Environmental 88, 232-239.

[13]Schmidt, W., et al., 2007. On the influence of ion exchange on the local structure of the titanosilicate ETS-10. Physical Chemistry Chemical Physics 9, 3440-3446.

[14]Howe, R.F., et al., 2005, Effects of Ion Exchange on the Structure of ETS-10. Chemical Materials 18, 928-933.

[15]Santamaria, J., et al., 2007. Preparation and Charactarisation of Titanosilicate Ag-ETS-10 for Propylene and Propane Adsorption 111, 4702-4709.

[16]Zhao, X.S., et al., 2009. Bactericidal activity of silver nanoparticles supported on microporous titanosilicate ETS-10. Microporous and Mesoporous Materials 120, 304-309.

[17]Zhu, L., Seff, K., 2009. Reinvestigation of the Crystal Structure of Dehydrated Sodium Zeolite X. Journal of Physical Chemistry B 013, 9512-9518.

[18]Pitman, R.N., et al., 1998. Next Generation Processes for NGL/LPG Recovery. Presented at the 77th Annual Convention of the GPA, 1-13.

[19]LeeSung-Hyun Kim, et al., 2008. Adsorption Equilibria of Methane, Ethane, Ethylene, Nitrogen, and Hydrogen onto Activated Carbon. Journal of Chemical and Engineering Data 48, 603-607.

[20]Brotas de Carvalho, M., et al., 2001. Adsorption of methane and ethane in zirconium oxide pillared clays. Separation and Purification Technology 21, 237-246.

[21]Khulbe, K.C., et al., 1996. Adsorption of methane, ethane, and ethylene on molecular sieve zeolites. Gas separation and purification 10, 81-84.

[22]Choudhary, V.R., Mayadevi, S., 1996. Adsorption of methane, ethane, ethylene, and carbon dioxide on Silicalite-1. Zeolites 17, 501-507.

[23]Cherbanski, R., Molga, E., 2009. Intensification of desorption processes by use of microwaves. An overview of possible applications and industrial perspectives. Chemical Engineering and Processing, 48, 1, 48-53

[24]Hashisho, Z., et al., 2005. Microwave-Swing Adsorption to Capture and Recover Vapours from Air Streams with Activated Carbon Fiber Cloth. Environmental Science and Technology 39, 6851-6859.

[25]Choudury, T,. et all. 2012. Regeneration of Na-ETS-10 using microwave and conductive heating. Chemical Engineering Science. (75). 282-288

[26]Choudury, T,. et all. 2013. Indirect and direct microwave regeneration of Na-ETS-10. Chemical Engineering Science. (95). 27-32

Chapter 2

C_2H_6 Recovery from a CH_4 Rich Stream on ETS-10 Materials

2.1 General Introduction

Annual global demand for C_2H_4, a precursor in the production of films, rubber and plastics, exceeds 100 million tonnes.[1] As the second largest component of raw natural gas (ranging from 0.7 to 6.8% by volume), C_2H_6 is commonly extracted for use as a petrochemical feedstock in the production of C_2H_4.[2] Current commercial technologies for extracting C_2H_6 from CH_4, the predominant combustible component of natural gas, are cryogenic and energy-intensive.[3] The development of selective adsorbents that can separate C_2H_6 from CH_4 at ambient temperature may lead to technologies that reduce the cost of C_2H_6 purification from natural gas liquids (NGL).

Currently, C_2H_6 is removed from CH_4 using cryogenic approaches. Conventional split vapour processes are reflux-based separations in which the > C2 hydrocarbon components of natural gas liquids are adsorbed and removed from raw natural gas by a gas sub-cooled approach, resulting in a split vapour stream.[4] Several improvements of this process have been developed over time in order to improve the recovery of > C2s and decrease energy consumption. Improvements such as extracting and sub-cooling a small portion of the residue

gas, supplying it to the top as feed and flashing it require capital investment, while the addition of a reflux through using the flashed split-vapour stream in a heat exchanger can reduce operating costs and improve propane recovery.[4] These methods effectively remove >C2s from natural gas, but the basic operational cost of the purification processes is high, and increases in separation efficiency are both incremental and capital-intensive. To be cost effective, the value of the extracted petrochemical feedstock (C_2H_6) must be greater than the sum of the extraction cost plus the value if the hydrocarbon were simply left in the gas stream.

Alternatives to traditional C_2H_6 extraction approaches include separation-based processes such as Pressure-Swing Adsorption (PSA) or Temperature-Swing Adsorption (TSA).[5] These processes use optimized adsorbents to separate gas mixtures based on the physical characteristics of their components. If an effective adsorbent could be identified that is selective for C_2H_6 over CH_4 at ambient temperature, the use of adsorptive separation might improve the economics of C_2H_6 purification.

Effective resolution of the smaller constituents of NGL, particularly the C2 species, would represent a significant improvement in adsorptive NGL separations. Engelhard Titanosilicate-10 (ETS-10) is a molecular sieve which can be modified to be highly selective for C_2H_6 over the CH_4, and would be an excellent candidate adsorbent for such a process.[7] ETS-10 is a large-pored, mixed octahedral/tetrahedral titanium silicate with a framework composed of a three-dimensional network of interconnecting channels and cavities.[8,9] The average

kinetic diameter of molecules able to enter the pores of ETS-10 is 8 Å, much larger than the kinetic diameters of C_2H_6 and CH_4, 4.44 Å and 3.76 Å, respectively.[10,11,12] However, ETS-10, like other molecular sieves, has a high ion exchange capacity associated with its framework: every titanium atom in the ETS-10 framework is counterbalanced by two univalent cations.[8,11,13] It has been predicted that the adsorption characteristics of ETS-10 can be manipulated through cation exchange in order to optimize both C_2H_6 capacity and C_2H_6/CH_4 selectivity.[7,14]

The objective of this work is to determine the potential utility of ETS-10, in its cation-exchanged forms, as an adsorbent for use in the separation of C_2H_6 from CH_4 at ambient temperature. In this study, we evaluate the adsorption of C_2H_6 and CH_4 on beds composed of Na-, Ba-, and Ba/H-ETS-10. Variation in selectivity between the three ion-exchanged forms of ETS-10 is attributed to changes in both the effective pore size and the strength of the adsorption sites upon ion exchange. The potential to design a swing adsorption process for the removal of C_2H_6 from a contaminated CH_4 stream is considered.

2.2 Experimental

2.2.1 Synthesis

Hydrothermal synthesis of ETS-10 was carried out.[8] A mixture of 50 g of sodium silicate (28.8% SiO_2, 9.14% Na_2O, Fisher), 3.2 g of sodium hydroxide (97% NaOH Fisher), 3.8 g of KF (anhydrous, Fisher), 4 g of HCl (1M), and 16.3 g of $TiCl_3$ solution (Fisher) was stirred in a blender for 1 h. The mixture was then

transferred to a Teflon-lined autoclave and reacted for 64 h at 488 K. The product was washed with deionised water and dried at 373 K.

Following drying, ETS-10 was reduced to a fine powder (<150 μm; 100 mesh) and total ion exchange was achieved by exposing the molecular sieve to an excess of $BaCl_2$ or NaCl in aqueous solution with stirring for 24 h at 373 K. Fully ion-exchanged ETS-10 was washed with deionised water and dried at 373 K. The mixed cationic form, Ba/H-ETS-10, was prepared through partial exchange with 6 meq/g of $BaCl_2$ followed by treatment in an HCl solution of pH 6 at 20°C for 16 h.

Samples were pelletized by mixing 2.5g of Ludox HS-40 colloidal silica (Aldrich) with 6 g of dried ETS-10, homogenizing with mortar and pestle, and compressing in a pellet press. The resulting discs were ground and sieved to a 20-50 mesh (297-841 μm).

2.2.2 Isotherm Measurement

Measurements of the single gas isotherms were performed through use of the Autosorb-1 MP volumetric adsorption unit equipped with a low pressure transducer (0-1 Torr) from Quantachrome (Boynton Beach, FL). All materials were degased at 523 K for 12 h under vacuum of greater than 10^{-4} Torr prior to adsorption tests.

The C_2H_6 and CH_4 isotherms were obtained for three cation-exchanged forms of ETS-10 (Na-, Ba-, and Ba/H-ETS-10) at 298K are shown in Figure 2.1. For C_2H_6, the most rectangular isotherm is observed on the Na-ETS-10 material. Ba-ETS-10 and Ba/H-ETS-10 C_2H_6 isotherms are progressively less rectangular,

indicating a weakening of adsorptive interactions, consistent with previous observations of ETS-10 materials.[14]

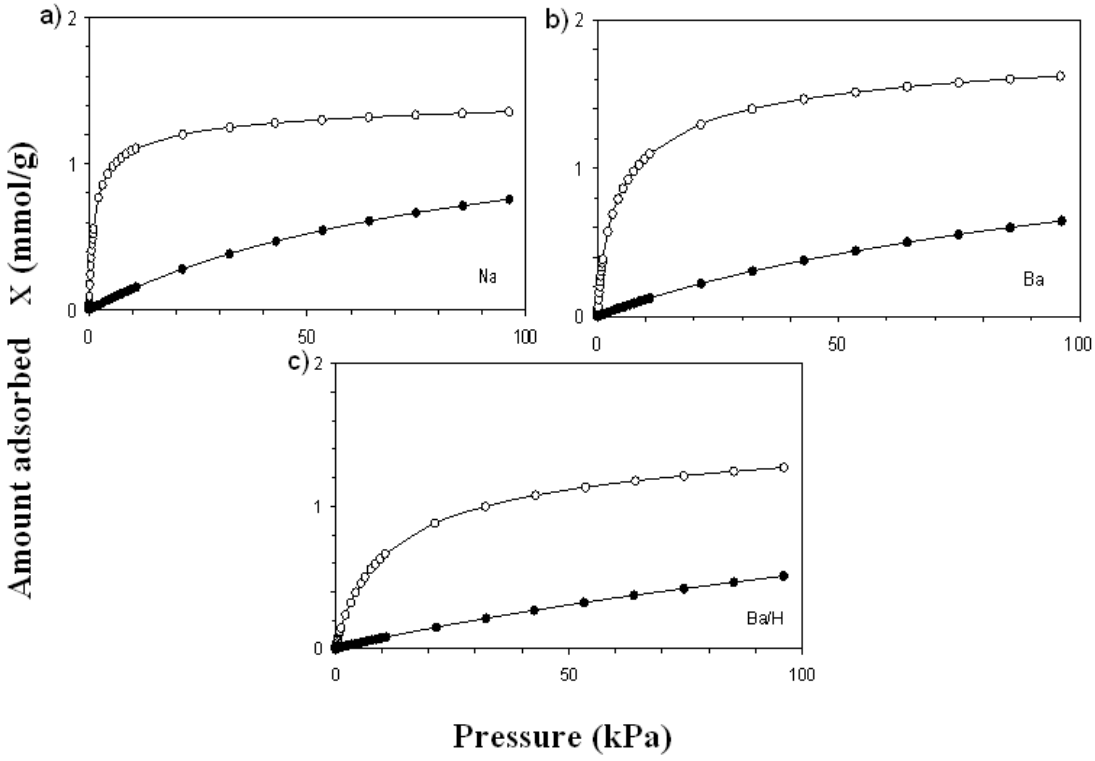

Figure 2.1: C_2H_6 (white circles) and CH_4 (black circles) adsorption isotherms at 298 K for three cation-exchanged forms of ETS-10; (a) Na-ETS-10, (b) Ba-ETS-10, (c) Ba/H-ETS-10.

Sorbate	Adsorbent	Saturation adsorption capacity x_m (mol/kg)	Equilibrium constant B x 10^2 (kPa^{-1})	Henry's law constant K_H x10^2 (mol/kg kPa)	Selectivity α (C_2H_6/CH_4)
CH_4	Na-ETS-10	1.47	1.1	1.6	54
	Ba-ETS-10	1.38	0.89	1.2	51
	Ba/H-ETS-10	1.58	0.49	0.78	22
C_2H_6	Na-ETS-10	1.32	63	83	N/A
	Ba-ETS-10	1.62	23	38	N/A
	Ba/H-ETS-10	1.39	8.8	12	N/A

Table 2.1: Adsorption parameters for C_2H_6 and CH_4 on ETS-10 materials at 298K.

The determination of the adsorbed amount of a single adsorbate gas on an adsorbent has been a common method to determine the effectiveness of gas separation since the development of surface adsorption models developed by Irving Langmuir. Gas adsorption within the pore spaces and on the surface is not limited to simply the Langmuir model. There are three basic models to the

equilibrium adsorption of single gasses, and they are the Langmuir approach, the Gibs approach, and the Potiential theory approach. In this work focus is put on the Langmuir model for its simplicity and ease of use. Determining the limiting selectivity from the Langmuir model is concise and gives a good description of the ability an adsorbent has in being more preferential toward one gas over another. In this model the amount of gas adsorbed x (mmol/g) onto an adsorbent surface and within the pore spaces of the adsorbent is measured against an increasing pressure P (KPa) of the specified gas.

Henry's constants follow the sequence: Na>Ba>Ba/H for both CH_4 and C_2H_6. The equilibrium constant for C_2H_6 on Na-ETS-10 (B), which has the most rectangular-shaped isotherm, was calculated to be 6.3×10^{-1} kPa^{-1}, whereas the Ba/H-ETS-10 isotherm, which approaches linearity, yields an equilibrium constant of 8.8×10^{-2} kPa^{-1}. Ba-ETS-10, which has a C_2H_6 isotherm of intermediate shape, also has an intermediate *B* value of 2.3×10^{-1} kPa^{-1}. Anson et all have made the same observations previously.[14] The *B* values for methane are much lower, ranging from 4.9×10^{-3} kPa^{-1} on Ba/H-ETS-10 to 1.1×10^{-2} kPa^{-1} on Na-ETS-10. Reflecting the nearly linear methane isotherms observed in Figure 2.1 the B values are understandable. The CH_4 isotherms are indicative of void filling by CH_4 within the ETS-10 materials, reflecting less adsorptive interaction between CH_4 and the sorbent in comparison to the C_2H_6 counterparts. The K_H values for each adsorbent/gas combination were used to calculate the limiting or Henry's selectivity (α) for C_2H_6 over CH_4 for the three materials in Table 2.1. The ranking of the different ETS-10 cation-exchanged forms, ranging from the most

selective to the least selective is: Na>Ba>Ba/H. The lowest selectivity is 22 (for Ba/H-ETS-10), while the Na-ETS-10 form has a limiting selectivity for C_2H_6 over CH_4 of 54 at 298 K.

2.2.3 Inverse Phase Chromatography (IPC)

The isotherms in Figure 2.1 display that the separation of the C_2H_6 from CH_4 is possible. IPC was utilized to demonstrate that a multicomponent mixture containing C_2H_6 from CH_4 can be separated into their constituent parts. In this experimental set up a column of 22.9 cm and diameter of 0.64 cm was packed with an as synthesized Na-ETS-10 material with no binder. The sample tube was then inserted into the GC oven and thermally activated to 523K under a He flow of 30 cc/min for 24 hr. Once activation was achieved the sample chamber was subjected to a pulse of 10 cc's of sample gas at a 50:50 composition of C_2H_6:CH_4. A pure sample of C_2H_6 and CH_4 were also tested. For each sample tested the oven temperature was raised to 343 K before the pulse was initialized and the resultant peaks from the TCD output as shown in Figure 2.2.

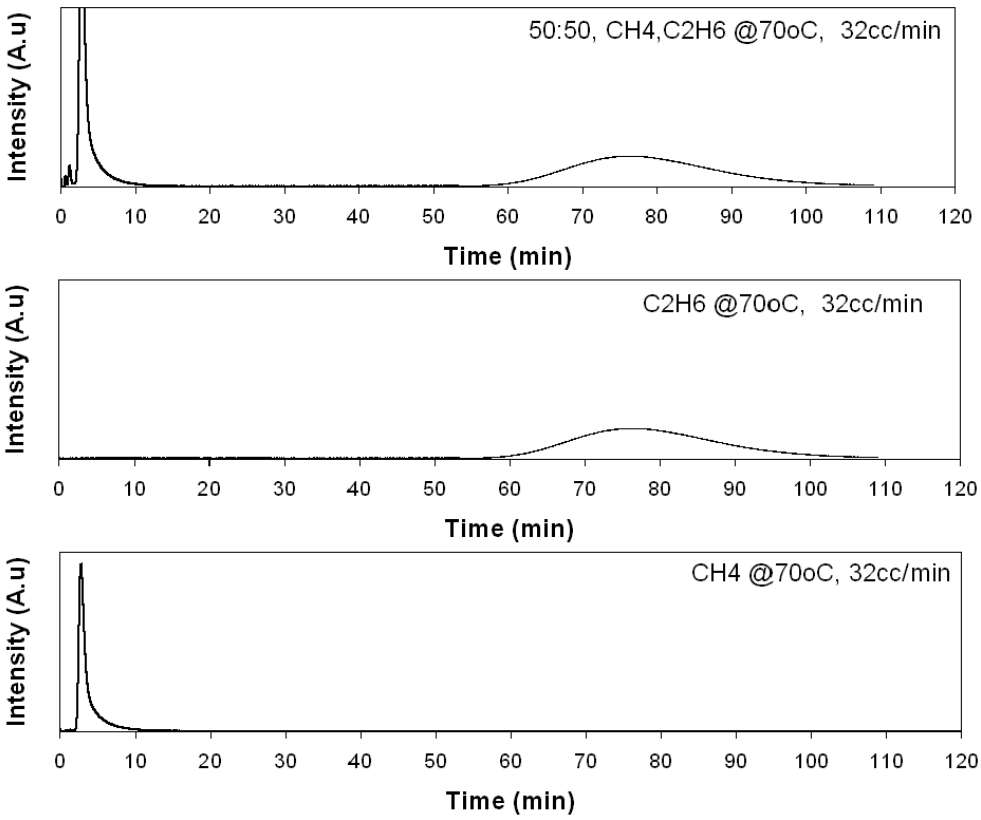

Figure 2.2: The inverse phase chromatography output at 343 K on Na-ETS-10 and at 32cc/min for a 50:50 mixture of CH_4 and C_2H_6, as well as the ouput for each single gas.

The IPC data in figure 2.2 shows that the separation of C_2H_6 and CH_4 is possible using Na-ETS-10. This adsorbent was selected due to having the highest α of the three exchanged forms studied in this work. A retention time of 78 min for C_2H_6 as compared to a retention time of 5 min for CH_4 shows that there is a much stronger adsorbing reaction of C_2H_6 this result is in agreement with the observations made above concerning figure 2.1 and the isotherm measurements.

2.2.4 *Experimental apparatus and adsorbent testing for breakthrough curves*

25 g samples of each test adsorbent were packed into a 40 cc cylindrical stainless steel tube with an outer diameter of 31.22 mm and a length of 75.59 mm. Packing densities for the Na, Ba and Ba/H forms were determined to be 0.824, 0.875, and 0.920 g/ml, respectively. Following adsorbent loading, columns were activated at 473 K for 10 h under 30 cm^3/min of helium flow. The gas was introduced into each test column at a gas flow rate of 170 ml/min. The in-house built adsorption unit is composed of a pressure gauge with a flow meter and needle valve to regulate flow, the packed column and the collection outlet. Samples were collected at the outlet of the column and transferred to the gas chromatograph at time intervals of 3 min. Gas chromatography (GC) analysis of outlet gas composition was performed using a Varian CP-3800 Gas Chromatograph equipped with a thermal conductivity detector.

Experimental set up was done as shown in Figure 2.3 where the sample gas, was a mock sample of natural gas. For the C_2H_6 breakthrough curves the sample gas composition shown in Table 2.2.

Gas constituent	% composition
CH_4	91
C_2H_6	5.6
C_3H_8	1.6
CO_2	0.7
N_2	0.5
C_4H_{10}	0.5
C_5H_{12}	0.1

Table 2.2 Gas constituents and % composition of the gas mixture used for the breakthrough curves measured.

GC data was processed using Microcal(TM) Origin^R Working Model Version 9.0 in order to determine the best fit using the Boltzmann equation. The breakthrough curves were measured using the sample gas mixture, the adsorbent column, and a bubble flow meter. The outlet gas composition was collected at 3 min intervals and manually transferred to the Gas chromatography setup. Figure 2.3 shows a IPC test for three different sections of the process. The input stream showing all constituents, the process stream void of C_2H_6 and higher molecular weight hydrocarbons, and the breakthrough stream with C_2H_6 present.

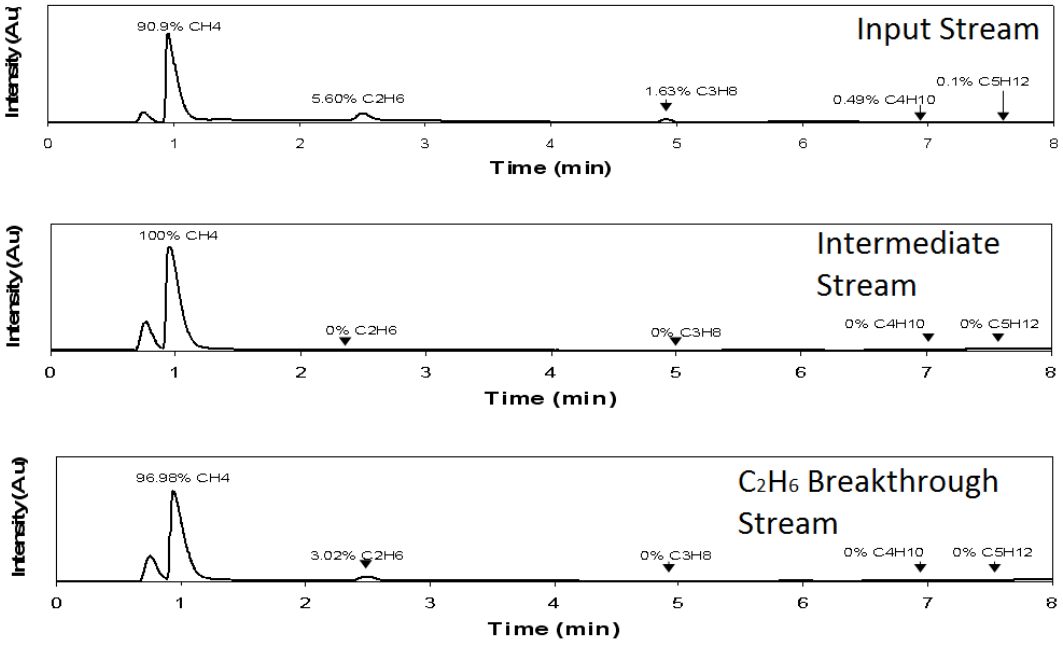

Figure 2.3 The G.C. output for the Input, Process, and Breakthrough streams for C_2H_6 removal from NGL's.

The N_2 is suspected to be a constituent of the pulse peak or the first peak in the chromatograph, and the CO_2 is suspected to be retained so strongly that it does not show up on our scale. The sample gas for each of the breakthrough testing procedures was passed through the adsorbent column with a 10mL/min flow rate. The outlet composition of the gas, was measured though use of a TCD detector. In C_2H_6 removal the more preferentially adsorbed species was C_2H_6.

As can be seen from Figure 2.3 the intermediate stream is void of all $C2^+$ components of the input stream. This shows that not only is the C_2H_6 removed from the input stream but also all components which have a higher carbon number. The first component of the $C2^+$ gasses that does breakthrough however is the C_2H_6 which is the fist indication that soon the C3, C4, and C5 components will breakthrough in succession afterward. The locations in the GC output that we

would expect C_2H_6, C_3H_8, C_4H_{10}, and C_5H_{12} to show up, shown on the intermediate output graph, but those peaks are absent due to being retained in the column. The bottom GC graph shows the composition of the outlet stream at the point of breakthrough of C_2H_6.

C_2H_6 breakthrough curves for Na-, Ba-, and Ba/H-ETS-10 are shown in Figure 2.4 and they follow the same trend as is seen in Table 2.2. Na-ETS-10 had the largest capacity for C_2H_6, 168 bed volumes. Bed volumes of 53 and 19 were observed for Ba-ETS-10 and Ba/H-ETS-10 breakthrough, respectively.The Na-ETS-10 shows the longest retention time and yielding the largest bed volume retention of C_2H_6 as well as the Ba/H and Ba forms following the same trend as observed above with the isotherm measurement in figure 2.1. This trend is Na>Ba>Ba/H. the Na form has the highest retention again due to the high interaction between C_2H_6 and the Na exchanged adsorption sites.

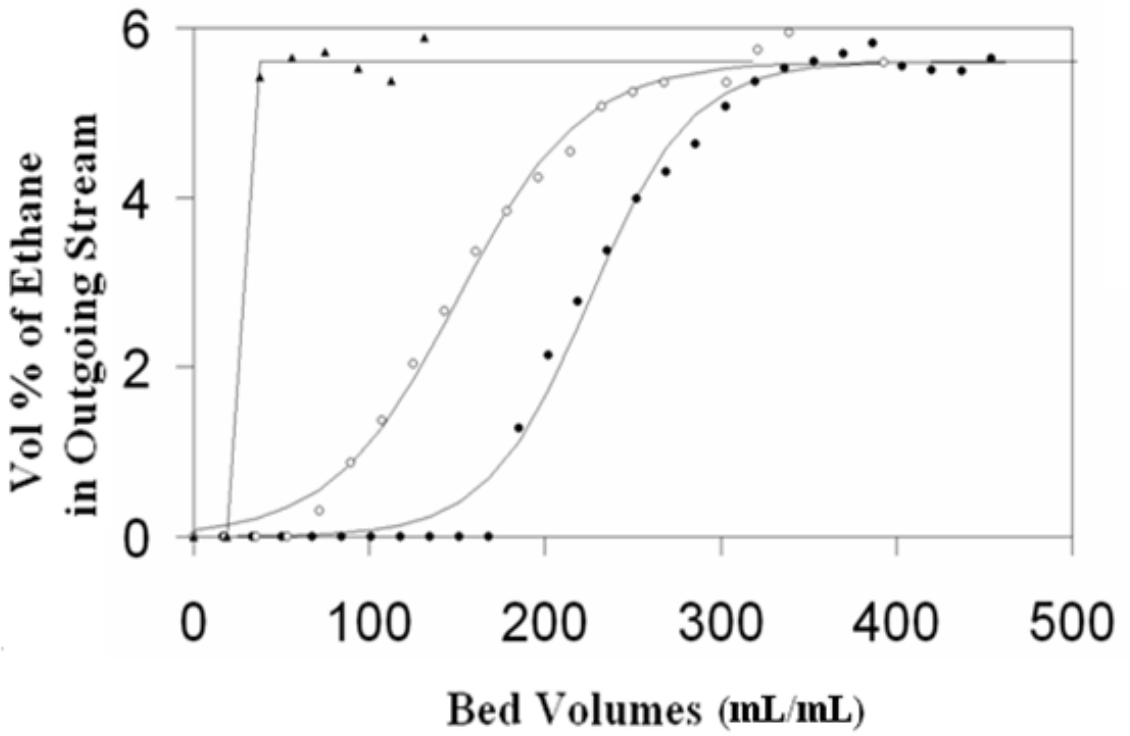

Figure 2.4 C_2H_6 adsorption breakthrough curves at 298K for three cation exchanged forms of ETS-10; a) Na-ETS-10 (black circles), b) Ba-ETS-10 (white circles), and c) Ba/H-ETS-10 (black triangles).

2.2.5 H_2O desorption and microwave regeneration

The H_2O desorption and microwave regeneration testing was performed using a conventional kitchen microwave which was retrofitted to accept an adsorbent column piped to be placed in its interior. The Na-ETS-10 adsorbent was selected for desorption testing due to its effectiveness in the removal C_2H_6 from CH_4 as observed in the isotherm measurement from figure 2.2 as well as the breakthrough curves shown in figure 2.3.

Sample preparation for the microwave regeneration testing was similar to the breakthrough testing above with some differences. 21 g samples of Na-ETS-10 was packed into a 32 cc cylindrical stainless steel tube. The column was activated at 473 K for 10 h under 30 cm^3/min of helium flow. The inlet stream mixture was of the same composition as table 2.2. An inlet stream of gas was introduced into the column at a gas flow rate of 170 ml/min. The set up for inlet gas addition, sample gathering, and microwave regeneration is shown in figure 2.5. A sample collected at the outlet of the column and transferred to the gas chromatograph at time intervals of 3 min. Gas chromatography (GC) analysis of outlet gas composition was performed using a Varian CP-3800 Gas Chromatograph equipped with a thermal conductivity detector.

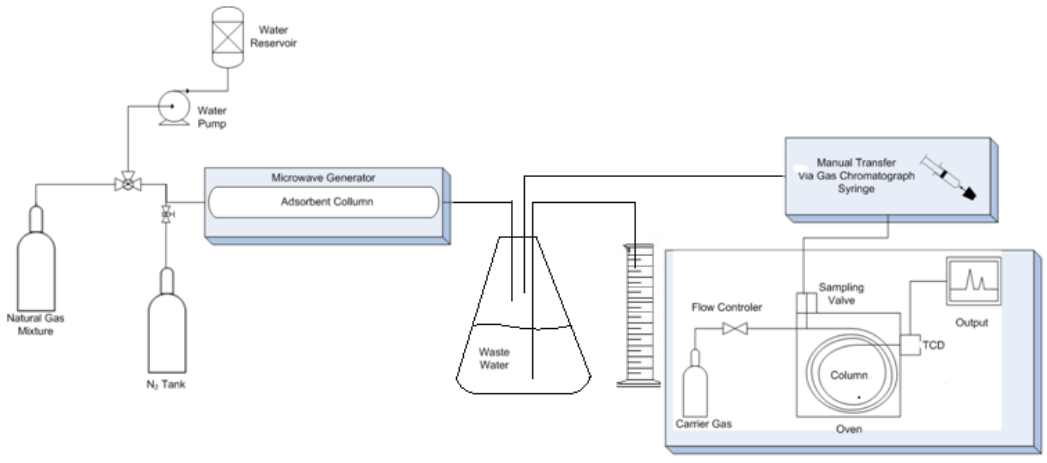

Figure 2.5 A process representation of the H_2O desorption and microwave regeneration unit, gas chromatography apparatus and adsorbent column.

Once the adsorbent bed had breakthrough reached C_2H_6 breakthrough at the outlet, the inlet stream adsorbed mixture was removed. The breakthrough was measured using manual transfer of the sample gas to the GC, the bed was saturated with a stream of water at 298K until breakthrough of water at the outlet of the column. The mixture of gasses that included the C_2+ gasses that were desorbed through being replaced with water, due to the greater capacity of the adsorbent for water, was sent to the G.C. for analysis. At this point the inlet of the column was subjected to a stream of N_2 at a flow rate of 500 cc/min which was applied to remove $H_2O_{(l)}$ from the spaces between and surface of adsorbent particles. Once $H_2O_{(l)}$ was no longer visible at the outlet the Quasar 800 Watt microwave was turned on for 6 min. Variable control of the output power of the microwave was used to raise up to and maintain an internal temperature of 220^oC. The internal temperature of the column was measured through use of a neoptix thermocouple fiber optic temperature sensor which was inserted into the column prior to saturation. As the internal temperature of the column was monitored the outlet of the column gas was collected. The outlet water vapor was collected over the interval of time required to raise the internal temperature of the adsorbent bed to 220^oC and disposed of. The volume of $H_2O_{(g)}$ desorbed was measured to indicate mass balance. Table 2.3 shows the values of heating time, volume of $H_2O_{(g)}$ desorbed, final temperature reached, time to breakthrough of C_2H_6, and volume of C_2H_6 desorbed.

Cycle	Volume of C_2H_6 Desorbed (ml)	Breakthrough Time (min)	Final Temp (K)	Volume of H2O Desorbed (ml)	Microwave Heating Time (min)	Bed Volumes (ml/ml)
1	653	69 +/- 10.2%	478	32.8	6	134
2	543.9	52 +/- 10.2%	502	32.8	6	100
3	878	49 +/- 10.2%	496	26.4	6	95

Table 2.3 The values of heating time, volume of $H_2O_{(g)}$ desorbed, final temperature reached, time to breakthrough of C_2H_6, and volume of C_2H_6 desorbed are shown.

After successive cycles the volume of C_2H_6 desorbed calculated from the volume of gas desorbed decreased with each cycle. This leads to a conclusion that there was insufficient regeneration. Additionally the bed volumes measured during this portion of the study were 25% lower than during the breakthrough portion to begin with during cycle 1. Either there were losses due to the inlet gas channeling due to upsets in the adsorbent bed structure, or inefficient microwave heating of the bed to remove adsorbed H_2O. Breakthrough times also decreased with successive testing

2.3 Conclusion

In this work, cation-exchanged forms of the titanosilicate ETS-10 are shown to be selective adsorbents for C_2H_6 over CH_4 at ambient temperature.

Three forms of ETS-10 (Na-, Ba-, and Ba/H-ETS-10) were compared in this study, and all three materials showed selectivity for C_2H_6 over CH_4 combined with C_2H_6 breakthrough capacities ranging from 19 to 168 bed volumes. The adsorption characteristics of cation-exchanged ETS-10 could be manipulated through the choice of cations. Na-ETS-10 combines the largest C_2H_6 capacity (168 mL/mL) with the highest limiting selectivity for C_2H_6 over CH_4 (α=63), of all the materials tested. Cation-exchanged ETS-10 has great potential for use as an adsorbent for the removal of C_2H_6 from natural gas streams. Adsorptive removal, likely through a pressure swing adsorption or temperature swing adsorption process, may reduce the cost of the purification of C_2H_6 from natural gas compared to conventional cryogenic separation techniques.

[1]Storck, W. J., 2006. Production: Growth is the Norm, Chemical and Engineering News 84, 59-68

[2]Rojey, A., Jaffret, C., 1997. Natural gas: production, processing, transport, Editions Technip, Paris

[3]Hinchliffe A.B., Porter K.E., 2000. A Comparison of Membrane Separation and Distilation. Chemical Engineering Research & Design 78, 255-268.

[4]Pitman, R.N., et al., 1998. Next Generation Processes for NGL/LPG Recovery. Presented at the 77th Annual Convention of the GPA, 1-13

[5]Maurer, R.T., Nanuet, N.Y., 1992. Methane purification by pressure swing adsorption. US Patent No. 51713335

[6]Yearout, J.D., 1969. Gas treating process and system. US Patent No. 3594983.

[7]Al-Baghli, N.N., Loughlin, K.F., 2006. Binary and Ternary Adsorption of Methane and Ethane and Ethylene on Titanosilicate ETS-10 Zeolite. Journal of Chemical Engineering Data, 51, 248-254.

[8]Kuznicki, S.M., 1991. Large-pored crystalline titanium molecular sieve zeolites. US Patent No. 5,011,591.

[9]Anderson, M.W., et al., 1994 Structure of the microporous titanosilicate ETS-10, Nature 367, 347-351.

[10]Breck, D.W., 1974. Zeolite Molecular Sieves: Structure, Chemistry and Use. Wiley-Interscience Publication, John Wiley & Sons, London.

[11]Hirschfelder, J.O., et al., 1954. In: Molecular Theory of Gases and Liquids. Wiley-Interscience Publication, John Wiley & Sons, New York

[12]Auerbach, S.M., Carrado K.A., 2003. Gas Separation by Zeolites, In: Handbook of Zeolite Science and Technology. Marcel Dekker Inc.

[13]Anderson, M.W., et al.,1999. Cation sites in ETS-10: Na-23 3Q MAS NMR and lattice energy minimisation calculations, Physical Chemistry Chemical Physics 1, 2287-2292.

[14]Anson A, et al., 2008. Adsorption of ethane and ethylene on modified ETS-10. Chemical Engineering Science 63, 4171-4175.

Chapter 3

H_2S Removal from a CH_4 Rich Stream on 13X, HiAl13X, and Complexation Materials

3.1 Introduction

NG is a variable gas formed during compression alterations of organic matter deep in the various layers of the earth beneath the surface. Its composition includes hydrocarbons such as (CH_4, C_2H_6, C_3H_8, C_4H_{10}, C_5H_{12}) and some non-hydrocarbon compounds (H_2, N_2, CO_2, H_2S). The contaminants listed are a natural component of all fossil fuels and cannot be avoided, and in some cases must be dealt with. Natural gas is a very environmentally friendly and relatively inexpensive fuel with high BTU. This resource can be used as fuel for vehicles, household purposes, and in industrial settings as precursors for reactions producing polymeric products. Some of these industrial products include organic acids, alcohols, and other organic compounds. Chemical composition of natural gas is quite different in different deposits there is a slight variation in the composition depending on its geographic location. Pollutants such as the non-hydrocarbon compounds mentioned above can vary as well. One such pollutant that is relevant to this paper is H_2S. Sulfur is present in natural gas as H_2S. The H_2S present is removed from the NG in specified refinery or gas plant process. Predominantly the removal of H_2S along with CO_2 contaminants is performed through gas adsorption into a liquid alkanolamine such as Monoethanolamine

(MEA) or Diethanolamine (DEA), which is a reversible process. This process is also known as gas sweetening.[1] This process is limited to high H_2S levels and is not 100% efficient therefore a finer removal step is sometimes needed. A generalization of the gas sweetening process shown in Figure 3.1. If the Sulfur in the H_2S is not removed it can be harmful to a process using a catalyst due to the heavy poisoning that results if the H_2S is not previously removed.[2] Sulfur poisoning on fuel cell electrodes is also an issue and this has been studied extensively.[3] When H_2S is dissolved in water it produces H_2SO_4 which is a strong acid and when this dissolution occurs in the atmosphere it produces acid rain. This acid rain is harmful to all life on the planet and in some areas it has devastated the fauna.[4]

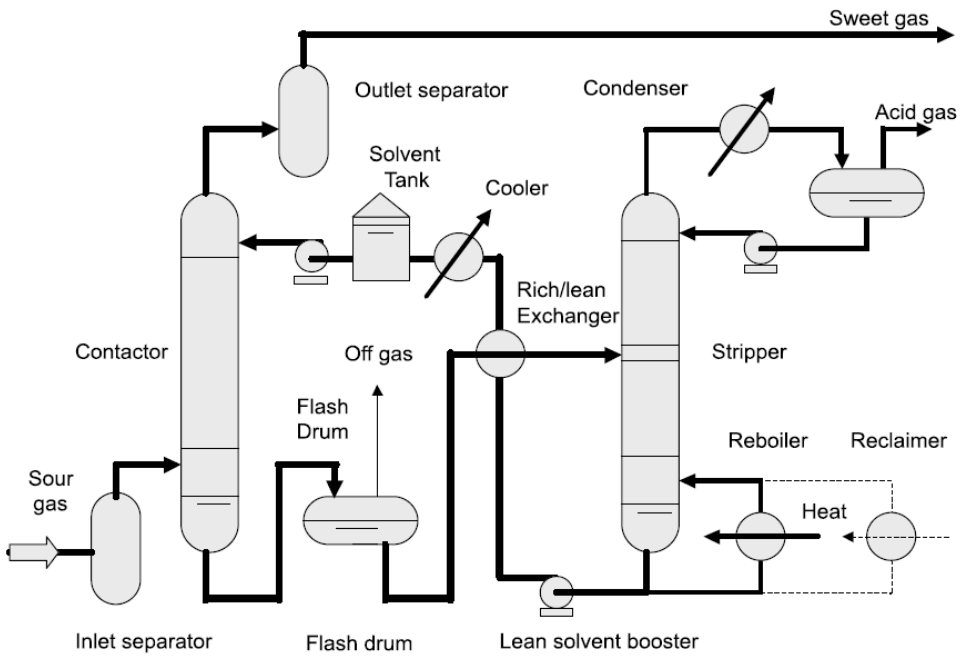

Figure 3.1 A process flow representation of the Gas Sweetening process that is currently widely employed in the Chemical and Petroleum Processing Industry.[1]

Gas adsorption of contaminants such as H_2S can be performed through use of tailored adsorbents in a fixed bed mode. ZnO is utilized currently at temperatures industrially with temperatures higher than 400K. Some studies have tried to apply ZnO onto graphite layers to reduce the temperature component to ambient, with little success.[2] Activated carbon with the addition of Bentonite Clay and Iron, Zinc and Copper Cation addition has been used to study H_2S adsorption.[4] Studies using activated carbon ground and mixed with 10% bentonite binders containing either iron, zinc or copper cations have been reported.[5] Other materials such as Zeolite 13X and Zinox 380 have been studied for their possible use as adsorbents in H_2S adsorption reactions.[6] This work did not use actual

natural gas streams but did characterise the above adsorbents as effective ad adsorbing H_2S. Caesium and Copper have been added to Zeolite Y and the adsorptive characteristics have been compared to Activated Carbon.[7] It was shown that the heavy metal materials had pronounced increases in capacity over the Activated Carbon. The adsorptive removal of Sulfur containing species has also been studied on materials such as Silver nitrate impregnated beta zeolite (BEA), mesoporous silica MCM-41 and SBA-15.[8]

Mechanisms of absorption where reactions are taking place and are irreversible, otherwise known as Chemisorption, have been studied for reactions with H_2S. Camille Petit et all have studied the chemisorption reactions between H2S and MOF's.[9] The H2S does react with the Cu-MOF quite strongly replacing water molecules. Metal-Sulfide nanoparticles have been produced on a Bentonite clay monolayer where H2S is the source of Sulfide.[10] The Metals used in this study were Lead and Zinc. These previous two examples show that heavy metals such as Copper, Lead, and Zinc can react strongly with H_2S. The aforementioned metals however have not been shown to have any irreversible or Physisorption interactions with H_2S.

The following is an overview of the color changes that occur as a result of reaction with H_2S with Pb, Cu, and Zn. The colour change when Lead is reacted with Hydrogen Sulfide is to a black color.[11] The zinc oxide reaction with H_2S produces a Black ZnS.[12] In Nature ZnS producing a black colour is present is a mineral called sphalerite. The product from a reaction between the copper(II) salts and H_2S produces a black colloidal precipitate of CuS.[13]

$$PbO_{(White)} + H_2S \rightarrow PbS_{(Brown)} + H_2O$$

$$ZnO_{(White)} + H_2S \rightarrow ZnS_{(Black)} + H_2O$$

$$Cu_2O_{(Light\ Blue)} + H_2S \rightarrow CuS_{\ (Black)} + H_2$$

3.2 Experiment and Discussion

H_2S removal capacity and breakthrough points of native Zeolite 13X, HiAl13X, Pb-13X, Cu-13X, and Zn-13X were all studied. Also a sample of Fe_2SO_4-CHA which was supplied to us from CCI Technologies was used to compare results. The H_2S adsorbents/reactants were measured at room temperature using a continuous flow system. High concentration of H_2S (1.5 v%) in CH_4. An on-line Gas Chromatograph with a TCD (Thermal Conductivity Detector) and a high sensitive SCD (Sulfur Chemiluminescence Detector) was used to continuously monitor the downstream H_2S concentration during the test. The experimental setup for H_2S removal adsorbents includes testing gas cylinder, inlet gas flowrate control and measurement, pressure indicator, H_2S adsorbent cartridge, outlet gas analysis and venting system shown in Figure 3.2.

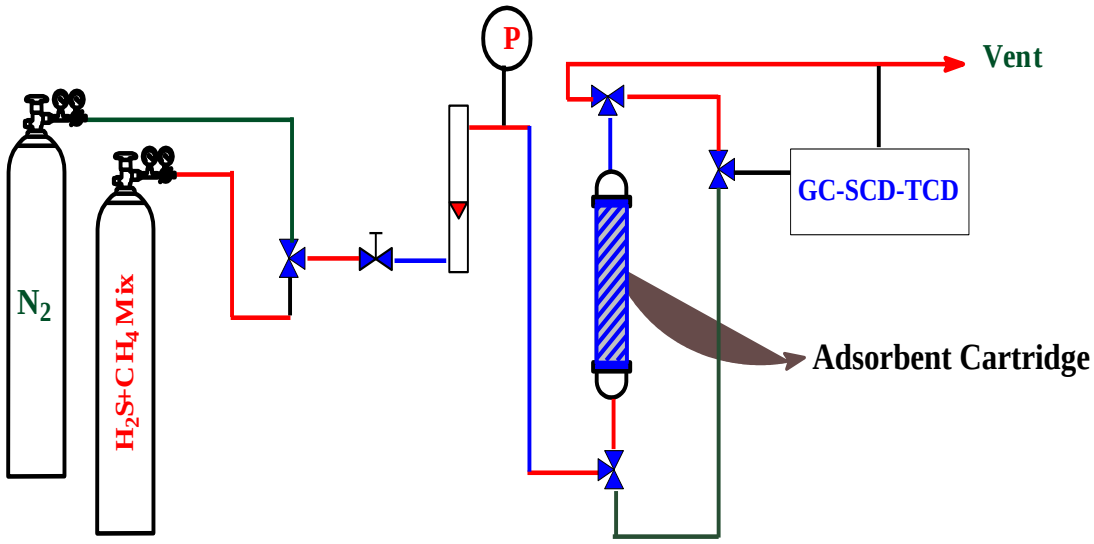

Figure 3.2 Schematics of the Novel H_2S Adsorbent Experimental Setup

The adsorbent cartridge/column used for testing was a stainless steel tube. The total packing volume of the column is 0.754mL for the 1.5% H_2S testing. All cation exchanged 13X adsorbents were prepared through a lab established exchange procedure with a corresponding metal salt solution followed filtration and drying at 80^{o}C. Before packing into the column all the adsorbents were ground to 25~50 mesh. Activation of the absorbent was performed in the column at 473K and flowing He gas at a flow rate of 30 cc/min. Downstream H_2S was analysed by an on-line GC equipped with a packed column (1/8" OD and 3 meter long) and a capillary column (0.28mm OD and 30 meter long) for CH_4 and H_2S analysis, respectively. A ten port gas sampling valve was used to inject gas sample from outlet line of the adsorbent column.

Before installation of the adsorbent column into the test system, a clean empty column of similar size was connected to the system. The system then was

purged with N2 at a flowrate of about 45mL/min until no trace of sulfur compound can be detected by the on-line GC-SCD. This GC-SCD has a sulfur detection limit of 5 ppbv. The following procedure was then implemented. First the empty column was changed to the testing column and check N_2 flow baseline, and then the inlet gas was switched from N_2 to H_2S in CH_4 mixture and adjusted to an adequate flow rate. The timer was then started once flow rate was established and stabilized; the outlet gas composition was then monitored through the on-line GC-TCD-SCD at time intervals necessary for breakthrough determination. Once the H_2S signal was detected by the SCD this indicated the H_2S breakthrough and hereafter the breakthrough profile was recorded until full breakthrough.

Due to the reaction between the metal exchanged sites on the Cu, Pb, and Zn forms of 13X there is a distinguished color change observed before and after breakthrough. All Ions form the sulfide when reacted with the H2S. Figure 3.3 shows the visible color change of unreacted and reacted adsorbent.

Figure 3.3 Visible Color Changes of the Metal Exchanged Complex Absorbents Before and After Breakthrough.

Breakthrough curves for the Pb, Zn, and Cu exchanged forms of 13x as well as Fe_2SO_4-CHA and the native form of 13X are shown in figure 3.4 and 3.5. Among the exchanged forms of 13X the volume of H_2S exposed to the adsorbent per cc of adsorbent shows that the Cu form of 13X has greatest capacity for H_2S as compared to the Pb form. The Zn form has the lowest capacity. Figure 3.3 shows the difference between the chemically modified form of 13X with higher Al content and the native form. This shows a significant increase in capacity for the HiAl form of 13X which is due to a greater number of adsorption sites. About 32.5% increase of H_2S capacity was achieved with a lab made chemically modified 13X adsorbent as compared to the commercial 13X counterpart.

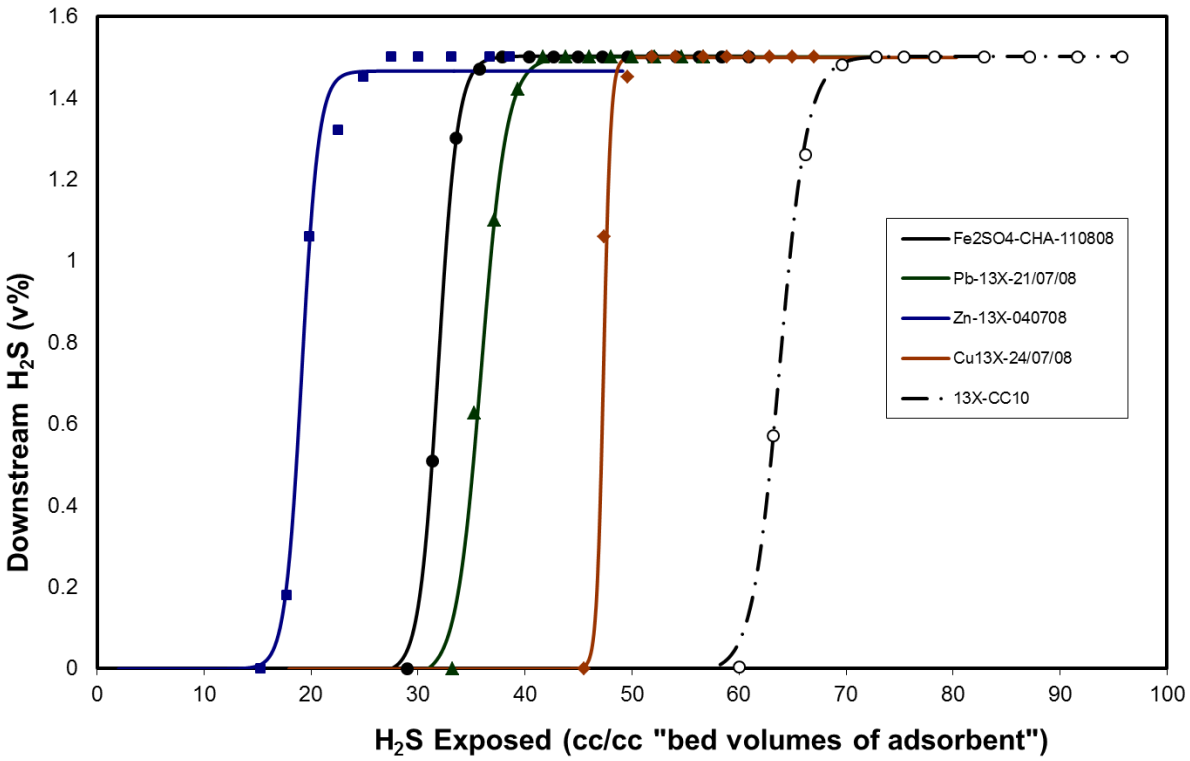

Figure 3.4 Breakthrough of H2S on the Metal Exchanged Complex Adsorbents Pb-13X, Zn-13X, Cu-13X, 13X, and Fe_2SO_4-CHA

The number of cation positions in the structure of 13X change from a Si/Al ratio of 1.3 to a ratio of 1.0 ideally in a high aluminum form. This was carried out in the lab through modifying the composition of the gel. This manipulation of the internal surface and chemical property of 13X produces more active cation sites that participate in adsorption. If there are a greater number of sites then there should in theory be a greater capacity before breakthrough. As is shown in figure 3.5 there is a marked increase in c0078z breakthrough amount of H_2S adsorbed. The breakthrough volume of H_2S adsorbed per cc of adsorbent changed from 63.16 cc/cc to 83.72 cc/cc once the increased Al form was tested.

Considering that the adsorbent binding sites are situated as the balancing charge for all AlO_4^- charges it stands to reason that with increased Al incorporated into the structure there would be more adsorption sites.

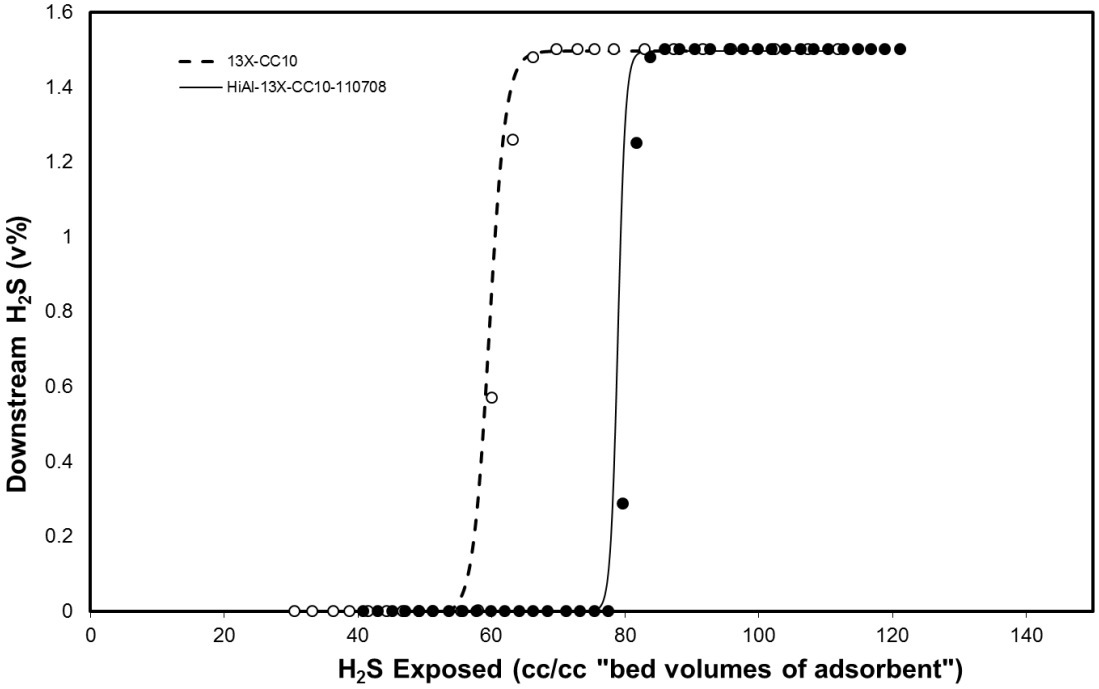

Figure 3.5 Improvement of H2S Adsorption Capacity of Chemically Modified HiAl-13X compared to Zeolite 13X at Room Temperature.

Table 3.1 shows a comparison of the breakthrough times and the capacity measured in cc's of H2S Adsorbed / cc of Column Packing. Also table 3.2 shows the boltzmann parameters calculated from the best fit curve to the boltzmann equation. It is evident that the removal of H_2S is much greater with the HiAl13X material when considering the outcome of fitting the data to the boltzmann equation. The value of $t_{1/2}$ for HiAl13X is 78.90 and when compared to the 13X $t_{1/2}$ value of 59.63 we notice that the HiAl13X has 32% greater capacity for H_2S.

When comparing the Metal exchanged materials the Cu material has the greatest $t_{1/2}$ value at 47.34.

Adsorbent	Time of Breakthrough (min)	cc's of H_2S Adsorbed / Column Packing at Breakthrough
Zeolite 13X	65.8	63.16
Pd-13X	39.40	35.27
Zn-13X	19.83	17.76
Cu-13X	52.93	47.39
HiAl-13X	93.52	83.72
Fe_2SO_4-CHA	35.02	31.35

Table 3.1 Summary of breakthrough time of metal exchanged Molecular sieve and natural zeolite adsorbents

Adsorbent	Boltzmann Equation Variables			
	Cg_1	Cg_2	$t_{1/2}$	M
Zeolite 13X	-1.05E-2	1.49	59.63	1.23
HiAl13X	-7.57E-4	1.49	78.90	0.56
Fe_2SO_4-CHA	-1.16E-2	1.50	31.89	0.89
Pb-13X	-2.27E-2	1.50	35.91	1.18
Zn-13X	-1.11E-3	1.46	19.13	0.78
Cu-13X	-1.02E-3	1.49	47.34	0.32

Table 3.1 Boltzmann equation variables for the data presented in Figures 3.3 and 3.4.

3.3 Conclusion

During the beginning stages of this work through literature review we assumed that there would be an increase in the adsorptive capacity of H_2S in the exchanged 13X. However this was not observed. Probing into the reasons for this would be a topic of future study. Determination of the internal structure and composition through SEM, as well as XRD would be the first step. Additional research could go into better understanding the parameters necessary for heavy metal exchange as well as how to obtain high coverage on the adsorbent of the heavy metals.

Through manipulation of the Aluminum content we did see an improvement in the adsorptive capacity of 32.5% in the HiAl13X. The Fe_2SO_4-CHA supplied by CCI Technologies as their chosen material did not perform as well as most of the test materials. The HiAl13X performed 167% better than the CCI Technologies material.

[1]GPSA Handbook., Section 21, Hydrocarbon Treating. Pages 21-1 to 21-34.

[2]Sung Chan Nam,. et all. 2013. Hydrogen sulfide adsorption on nono-sized zinc oxide/reduced graphite oxide composite at ambient condition. Applied Surface Science. (276) 646-652

[3]Weidner,. J.W,. et all. 2010. Analysis of sulfur poisoning on a PEM fuel electrode. Electrochmical Acta. (55). 5683-5694

[4]Paloma, H, et all,. 2004. Catalytic combustion of methane over commercial catalysts in presence of ammonia and hydrogen sulphide. Chemosphere (55). 681–689

[5]Nguyen-Tanh, D., Bandosz, J.T,. 2004. Activated carbons with metal containing bentonite binders as adsorbents of hydrogen sulfide. Carbon (43), 359-367

[6]Melo, D.M.A. et all., 2006. Evaluation of Zinox and Zeolite materials as adsorbents to remove H_2S from natural gas. Colloids and Surfaces A: Physicochem Eng Aspects 272 32-36

[7]Israelson, G, et all,. 2006. Regenerable Sorbent for Natural Gas Desulfurization. Journal of Materials Engineering and Performance Vol 15(4). 433-438

[8]Jong-Nam Kim et all., 2007. Selective removal of sulfur compounds in city gas by adsorbents. Korean Journal of Chemical Engineering., 24(6), 1124-1127

[9]Camille, P, et all,. 2012. Reactive adsorption of acidic gases on MOF/graphite oxide composites. Microporous and Mesoporous Materials. (154). 107–112

[10]Lubos Jankovic, et all,. 2010. Synthesis and characterization of low dimensional ZnS- and PbS-semiconductor particles on a montmorillonite template. Physical Chemistry Chemical Physics. 12, 14236–14244

[11]Patnaik, Pradyot (2003). Handbook of Inorganic Chemical Compounds. McGraw-Hill. ISBN 0-07-049439-8. Retrieved 2009-06-06.

[12]Wells, A. F. (1984), Structural Inorganic Chemistry (5th ed.), Oxford: Clarendon Press, ISBN 0-19-855370-6

[13]Greenwood, Norman N.; Earnshaw, Alan (1997). Chemistry of the Elements (2nd ed.). Butterworth-Heinemann. ISBN 0080379419.

Chapter 4: Summary

4.1 CH_4/C_2H_6 Separation

ETS-10 exchanged materials have shown in this work that they are effective at the separation of CH_4 and C_2H_6. The capacities of the Ba and Ba/H forms of the ETS-10 did not perform as well as the Na form. Considering that many materials have been used for Pressure Swing Adsorption or Temperature Swing Adsorption systems it would be interesting to determine which material would perform better under industrial conditions. One aspect of adsorption that would need to be taken into account is how strongly the gas adsorbs to the surface or pore space. Taking into account Figure 2.1 it is evident that the strength of adsorption or the Heat of Adsorption ΔH, is much greater for the Na and Ba forms of the ETS-10 than the Ba/H. This alludes to the possibility that the Ba/H form may be better for a PSA process considering the removal of the C_2H_6 may be easier to remove from the adsorbent.

Microwave desorption is an effective method for the removal of adsorbed species onto the adsorbent surface. A system that employed the removal of gasses from the surface of a material in an industrial setting would be much larger than the equipment employed during this work. One major concern would be safety around a device that enabled desorption of gasses using microwaves with industrial sized columns.

4.2 H_2S Adsorption Materials for Natural Gas Streams

This work has shown that improvements on current commercial H_2S scrubbing products can be made from relatively low cost precursors. Materials such as Zeolite 13X (NaX), HiAl13X, Cu13X, Pd13X, and Zn13X . With H_2S being a poisoning agent on the surface of a catalyst a guard bed cold be utilized to remove the H_2S before the natural gas is exposed to the catalyst. Through removing the H_2S inline and at room temperature this would create a measurable increase in catalyst lifetime, without the need to high temperatures using ZnO. These guard beds would need to be disposed of as the H_2S is adsorbed so strongly to the extent of chemisorption. The next concern is to create a system that can remove the H_2S reversibly and be able to swing the system to desorb and regenerate the adsorbent. Aspects taken into account in a study on the regenerability would be investigating the chemisorption environment, and possibly reacting the Sulfur with a stream of gas to that would reduce the Sulfur to a gas and desorb or push the chemisorbed reaction back to the starting point.